Chapter 10
Spherically Symmetric Potentials: Radial Equation

Now that we have studied angular momentum, it is an easy matter to obtain a solution of the Schrödinger equation for spherically symmetric potentials $V(r)$. I will look at bound state solutions of Schrödinger's equation for the infinite spherical well potential, the finite spherical well potential, the Coulomb potential (hydrogen atom), and the isotropic, 3-D harmonic oscillator potential. Among these, the Coulomb potential is undoubtedly the most important, since the solution of the Coulomb problem was one of the major triumphs of quantum mechanics.

To help understand the quantum bound state radial probability distributions, it will be helpful to compare the quantum results with the classical radial probability distributions. For a particle having mass μ moving in a potential $V(r)$, the effective potential is

$$V_{\text{eff}}(r) = V(r) + L^2/\left(2\mu r^2\right), \tag{10.1}$$

where L is the magnitude of the angular momentum of the particle. For the effective potentials that I discuss (see, for example, Fig. 10.1), the bound state classical motion is always restricted to a range $r_{\min} \leq r \leq r_{\max}$, where the values of $r_{\min}$ and $r_{\max}$ are classical *radial turning points* of the orbits for a given energy and angular momentum (for $L = 0$, the classical orbit is a bounded straight line though the origin, but $r_{\min} = 0$ is still a turning point for the *radial* motion). In this chapter I use the symbol μ for the mass to distinguish it from the magnetic quantum number m—it has the added advantage that in two-body problems such as hydrogen, μ actually refers to the reduced mass of the electron.

I define a time T_{21} as the time it takes for a classical particle having mass μ to move from $r_{\min}$ to $r_{\max}$. In the case of the Coulomb and oscillator potentials, the bound orbits are *closed*. The time T_{21} is half the orbital period in the Coulomb problem and one-quarter the orbital period in the oscillator problem. For other

P.R. Berman, *Introductory Quantum Mechanics*, UNITEXT for Physics,
https://doi.org/10.1007/978-3-319-68598-4_10

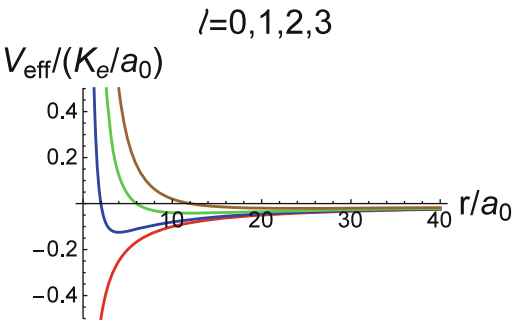

Fig. 10.1 Effective potential for the Coulomb potential, $V(r) = -K_e/r$ in units of K_e/a_0 as a function of r/a_0, where a_0 is the Bohr radius. To relate the classical and quantum problems, the angular momentum is set equal to $\hbar\sqrt{\ell(\ell+1)}$. The lowest curve has $\ell = 0$ and the other curves are in order of increasing ℓ

potentials the motion is *not* periodic and the orbits, while bound, are not closed. I assume that there is a single $r_{\min}$ and a single $r_{\max}$ in the effective potential for each energy.

The *classical radial probability distribution* is equal to the time the particle spends in an interval dt during its motion between $r_{\min}$ and $r_{\max}$, divided by T_{21}, namely

$$P^{\text{class}}(r)\,dr = \frac{|dt|}{T_{21}} = \frac{1}{T_{21}}\left|\frac{dt}{dr}\right| dr. \tag{10.2}$$

I use conservation of energy to calculate $|dt/dr|$. The energy in the classical case can be written as

$$E = \frac{\mu}{2}\left(\frac{dr}{dt}\right)^2 + \frac{L^2}{2\mu r^2} + V(r). \tag{10.3}$$

From this equation, it follows that

$$\frac{dt}{dr} = \frac{1}{\sqrt{\frac{2}{\mu}\left(E - V(r) - \frac{L^2}{2\mu r^2}\right)}}, \tag{10.4}$$

which implies that

$$T_{21} = \int_{r_{\min}}^{r_{\max}} \frac{dr}{\sqrt{\frac{2}{\mu}\left(E - V(r) - \frac{L^2}{2\mu r^2}\right)}}. \tag{10.5}$$

Combining Eqs. (10.2), (10.4), and (10.5), I find

$$P^{\text{class}}(r) = \frac{1}{T_{21}\sqrt{\frac{2}{\mu}\left(E - V(r) - \frac{L^2}{2\mu r^2}\right)}}$$
$$= \frac{1}{\sqrt{\frac{2}{\mu}\left(E - V(r) - \frac{L^2}{2\mu r^2}\right)}\int_{r_{\min}}^{r_{\max}} \frac{dr}{\sqrt{\frac{2}{\mu}\left(E - V(r) - \frac{L^2}{2\mu r^2}\right)}}}, \tag{10.6}$$

where $r_{\min}$ and $r_{\max}$ are the solutions of the equation

$$V_{\text{eff}}(r_{\min,\max}) = V(r_{\min,\max}) + \frac{L^2}{2\mu r_{\min,\max}^2} = E. \tag{10.7}$$

The effective potential is extremely useful in analyzing problems involving central forces. For example, consider the attractive Coulomb problem for which the potential energy is

$$V(r) = -\frac{K_e}{r}, \tag{10.8}$$

where K_e is a positive constant. The effective potential is drawn in Fig. 10.1 for several angular momenta. Classically, if the particle has negative energy, $E < 0$, it is always bound. For $L = 0$ the particle orbit passes through the center of force and the energy can go to $-\infty$. For any $L > 0$, the particle can never go through the origin and the particle must have a minimum energy $E_{\min}$ that can be obtained by setting $dV_{\text{eff}}(r)/dr = 0$. For $L > 0$ and $E_{\min} \leq E < 0$, the classical orbit is *bound* between the two radii $r_{\min,\max}$. At such turning points in the orbit, the *radial* kinetic energy vanishes.

If the angular momentum is zero, the orbit passes through the origin and all the kinetic energy arises from its radial component. At points where the effective potential has a minimum, the particle undergoes circular motion and all the kinetic energy arises from the angular motion. If we fix the energy in bound state problems, there is a maximum value of the angular momentum determined by

$$\frac{1}{2}\frac{L_{\max}^2}{\mu r_0^2} = E - V(r_0), \tag{10.9}$$

where r_0 is the value of the radius for which the effective potential is a minimum. On the other hand, if instead of fixing the energy we fix the angular momentum and if $L > 0$, then the energy of the particle must be greater than or equal to some minimum energy,

$$E_{\min} = V(r_0) + \frac{1}{2}\frac{L^2}{\mu r_0^2}, \tag{10.10}$$

since there is a non-vanishing component of the kinetic energy resulting from the angular motion.

In quantum mechanics there is something analogous to the radial momentum defined in Eq. (9.10), allowing us to reduce the quantum problem to an effective one-dimensional problem for the radial motion. The effective potential serves as the potential for this one-dimensional radial motion. For example, we can expect that there may be bound state motion for $E < 0$ for the Coulomb effective potential shown in Fig. 10.1. However, for $L = 0$, we do not expect the minimum energy to equal $-\infty$ and, for any $L \neq 0$, we expect that, *if* there are bound states for a given L, the minimum energy will be larger than the minimum energy of the classical problem. The particle cannot rest at the minimum of the effective potential since this would violate the uncertainty principle. As in the classical problem, for a given bound state energy, there will be a maximum value of the magnitude of the angular momentum that is allowed.

10.1 Radial Momentum

The classical Hamiltonian is given by

$$H_{\text{class}} = \frac{p_r^2}{2\mu} + \frac{L^2}{2\mu r^2} + V(r), \tag{10.11}$$

where

$$p_r = \frac{\mathbf{p} \cdot \mathbf{r}}{r}, \tag{10.12}$$

is the radial component of the momentum. On the other hand, the quantum Hamiltonian is

$$\hat{H} = \frac{\hat{p}^2}{2\mu} + \hat{V} = -\frac{\hbar^2}{2\mu}\nabla^2 + V(r). \tag{10.13}$$

Writing ∇^2 in spherical coordinates,

$$\nabla^2 = \frac{1}{r^2}\frac{\partial}{\partial r}r^2\frac{\partial}{\partial r} + \frac{1}{r^2\sin\theta}\frac{\partial}{\partial\theta}\sin\theta\frac{\partial}{\partial\theta} + \frac{1}{r^2\sin^2\theta}\frac{\partial^2}{\partial\phi^2}, \tag{10.14}$$

and using the fact that

$$\hat{L}^2 = -\hbar^2\left[\frac{1}{\sin\theta}\frac{\partial}{\partial\theta}\sin\theta\frac{\partial}{\partial\theta} + \frac{1}{\sin^2\theta}\frac{\partial^2}{\partial\phi^2}\right], \tag{10.15}$$

I can rewrite the quantum Hamiltonian as

$$\hat{H} = -\frac{\hbar^2}{2\mu}\left(\frac{1}{r^2}\frac{\partial}{\partial r}r^2\frac{\partial}{\partial r}\right) + \frac{\hat{L}^2}{2\mu r^2} + V(r). \tag{10.16}$$

If you compare Eqs. (10.11) and (10.16), it would seem that

$$\hat{p}_r^2 = -\hbar^2 \left(\frac{1}{r^2} \frac{\partial}{\partial r} r^2 \frac{\partial}{\partial r} \right), \tag{10.17}$$

but this is not guaranteed. I must obtain an expression for the quantum-mechanical radial momentum operator corresponding to the classical variable given in Eq. (10.12) to show whether or not this is the case. To get an Hermitian operator that corresponds to this classical variable, I take the symmetrized form

$$\hat{p}_r = \frac{1}{2} \left(\frac{\mathbf{r}}{r} \cdot \hat{\mathbf{p}} + \hat{\mathbf{p}} \cdot \frac{\mathbf{r}}{r} \right) = \frac{\hbar}{2i} \left(\mathbf{u}_r \cdot \boldsymbol{\nabla} + \boldsymbol{\nabla} \cdot \mathbf{u}_r \right). \tag{10.18}$$

I next evaluate

$$\begin{aligned} \hat{p}_r \psi &= \frac{\hbar}{2i} \left[\mathbf{u}_r \cdot \boldsymbol{\nabla} \psi + \boldsymbol{\nabla} \cdot (\mathbf{u}_r \psi) \right] \\ &= \frac{\hbar}{2i} \left[\frac{\partial \psi}{\partial r} + \psi \boldsymbol{\nabla} \cdot \mathbf{u}_r + \mathbf{u}_r \cdot \boldsymbol{\nabla} \psi \right] \\ &= \frac{\hbar}{2i} \left[2 \frac{\partial \psi}{\partial r} + \psi \boldsymbol{\nabla} \cdot \mathbf{u}_r \right]. \end{aligned} \tag{10.19}$$

To calculate $\boldsymbol{\nabla} \cdot \mathbf{u}_r$, I use spherical coordinates,

$$\boldsymbol{\nabla} \cdot \mathbf{u}_r = \frac{1}{r^2} \frac{\partial}{\partial r} r^2 = \frac{2}{r}. \tag{10.20}$$

It then follows that

$$\hat{p}_r = \frac{\hbar}{i} \left(\frac{\partial}{\partial r} + \frac{1}{r} \right) \tag{10.21}$$

and

$$\begin{aligned} \hat{p}_r^2 \psi &= -\hbar^2 \left(\frac{\partial}{\partial r} + \frac{1}{r} \right) \left(\frac{\partial \psi}{\partial r} + \frac{\psi}{r} \right) \\ &= -\hbar^2 \left[\frac{\partial^2 \psi}{\partial r^2} + \frac{2}{r} \frac{\partial \psi}{\partial r} - \frac{\psi}{r^2} + \frac{\psi}{r^2} \right] \\ &= -\hbar^2 \left[\frac{\partial^2 \psi}{\partial r^2} + \frac{2}{r} \frac{\partial \psi}{\partial r} \right] = -\hbar^2 \left(\frac{1}{r^2} \frac{\partial}{\partial r} r^2 \frac{\partial \psi}{\partial r} \right), \end{aligned} \tag{10.22}$$

or

$$\hat{p}_r^2 = -\hbar^2 \left(\frac{1}{r^2} \frac{\partial}{\partial r} r^2 \frac{\partial}{\partial r} \right). \tag{10.23}$$

Combining Eqs. (10.16) and (10.23), I find

$$\hat{H} = \frac{\hat{p}_r^2}{2\mu} + \frac{1}{2}\frac{\hat{L}^2}{\mu r^2} + \hat{V}, \tag{10.24}$$

which mirrors the classical Hamiltonian given in Eq. (10.11).

[As an aside, I might point out the situation is *different* for problems with cylindrical symmetry about the z-axis. The classical Hamiltonian for two-dimensional motion in the xy plane is

$$H_{\text{class}} = \frac{p_\rho^2}{2\mu} + \frac{L_z^2}{2\mu\rho^2} + V(\rho), \tag{10.25}$$

where ρ is a cylindrical coordinate and $p_\rho = \mathbf{p}\cdot\mathbf{u}_\rho$. The corresponding quantum Hamiltonian is

$$\hat{H} = -\frac{\hbar^2}{2\mu}\nabla^2 + V(\rho) = -\frac{\hbar^2}{2\mu}\left(\frac{1}{\rho}\frac{\partial}{\partial\rho}\rho\frac{\partial}{\partial\rho}\right) + \frac{\hat{L}_z^2}{2\mu\rho^2} + V(\rho), \tag{10.26}$$

which would suggest that

$$\hat{p}_\rho^2 = -\hbar^2\left(\frac{1}{\rho}\frac{\partial}{\partial\rho}\rho\frac{\partial}{\partial\rho}\right) \tag{10.27}$$

in the quantum case, but this is **not** true. Instead, (see problems)

$$\hat{p}_\rho^2 = -\hbar^2\left(\frac{1}{\rho}\frac{\partial}{\partial\rho}\rho\frac{\partial}{\partial\rho}\right) + \frac{\hbar^2}{4\rho^2}, \tag{10.28}$$

and the effective potential in the quantum problem is

$$\hat{V}_{\text{eff}} = \hat{V} + \frac{\hat{L}_z^2}{2\mu\rho^2} - \frac{\hbar^2}{8\mu\rho^2}. \tag{10.29}$$

There is an attractive quantum correction, $-\hbar^2/8\mu\rho^2$, to the classical effective potential.]

10.2 General Solution of the Schrödinger Equation for Spherically Symmetric Potentials

The time-independent Schrödinger equation that must be solved is

$$\hat{H}\psi_E(\mathbf{r}) = \left[-\frac{\hbar^2}{2\mu}\nabla^2 + V(r)\right]\psi_E(\mathbf{r}) = E\psi_E(\mathbf{r}) \tag{10.30}$$

or

$$\frac{\hbar^2}{2\mu}\left(\frac{1}{r^2}\frac{\partial}{\partial r}r^2\frac{\partial\psi_E(\mathbf{r})}{\partial r}\right)+\left[E-V(r)-\frac{\hat{L}^2}{2\mu r^2}\right]\psi_E(\mathbf{r})=0. \tag{10.31}$$

Based on the fact that $\hat{H}$, $\hat{L}^2$, and $\hat{L}_z$ commute and that the $Y_\ell^m(\theta,\phi)$ are simultaneous eigenfunctions $\hat{L}^2$ and $\hat{L}_z$, I try a solution of the form

$$\psi_{E\ell m}(\mathbf{r})=R_{E\ell}(r)Y_\ell^m(\theta,\phi), \tag{10.32}$$

substitute it into Eq. (10.31), and use the fact that

$$\hat{L}^2Y_\ell^m(\theta,\phi)=\hbar^2\ell(\ell+1)Y_\ell^m(\theta,\phi) \tag{10.33}$$

to obtain

$$\begin{aligned}&\frac{\hbar^2}{2\mu}\left(\frac{1}{r^2}\frac{d}{dr}r^2\frac{dR_{E\ell}(r)}{dr}\right)+\left[E-V(r)-\frac{\hbar^2\ell(\ell+1)}{2\mu r^2}\right]R_{E\ell}(r)=0;\\ &\frac{d^2R_{E\ell}(r)}{dr^2}+\frac{2}{r}\frac{dR_{E\ell}(r)}{dr}+\frac{2\mu}{\hbar^2}\left[E-V(r)-\frac{\hbar^2\ell(\ell+1)}{2\mu r^2}\right]R_{E\ell}(r)=0.\end{aligned} \tag{10.34}$$

Using the results of Chap. 9, I have shown that it is a simple matter to reduce all central field problems to the solution of a *one-dimensional radial equation* for the *radial wave function* $R_{E\ell}(r)$. Note that the radial wave function has units of volume$^{-3/2}$.

Let's pause for a second and appreciate the importance of Eq. (10.34). We see that, *for each value* of ℓ, there is a radial equation that must be solved for an effective potential

$$V_{\text{eff}}(r)=V(r)+\frac{\hbar^2\ell(\ell+1)}{2\mu r^2}. \tag{10.35}$$

That is, for each value of ℓ, we can determine what bound states, if any, are present. *It is helpful to remember that each value of ℓ, in effect, corresponds to a separate problem for a given central force field.* You see that the magnetic quantum number m of $Y_\ell^m(\theta,\phi)$ does not appear in Eq. (10.34). Owing to the spherical symmetry of the potential, the energy depends only on the magnitude of the angular momentum and *not* on its direction. In the classical problem, this leads to an infinite degeneracy since all directions of $\mathbf{L}$ are allowed. In quantum mechanics, however, the degeneracy is discrete since, for each value of ℓ, m can take on $(2\ell+1)$ values $[-\ell,-\ell+1,\ldots\ell-1,\ell]$. In other words, owing to spherical symmetry, the eigenfunctions $\psi_{E\ell m}(\mathbf{r})$ are at *least* $(2\ell+1)$-fold degenerate for a given value of E and ℓ.

It is sometimes convenient to introduce a function

$$u_{E\ell}(r) = rR_{E\ell}(r) \tag{10.36}$$

which transforms Eqs. (10.34) into

$$\frac{d^2u_{E\ell}(r)}{dr^2} + \frac{2\mu}{\hbar^2}\left[E - V(r) - \frac{\hbar^2\ell(\ell+1)}{2\mu r^2}\right]u_{E\ell}(r) = 0. \tag{10.37}$$

From here onwards, I usually drop the E subscript—it is implicit.

10.2.1 Boundary Conditions

As in any problem in quantum mechanics, we must examine the boundary conditions. It is assumed that $V(r) > E$ as $r \to \infty$, since the discussion is restricted to bound states. As such, I expect the radial wave function to fall off exponentially as some power of the radius as $r \to \infty$ since $r \to \infty$ corresponds to the classically forbidden region (a region where the radial contribution to the kinetic energy is negative). The exact form of the dependence depends on the nature of the potential, but the centrifugal (angular momentum term) potential does not contribute as $r \to \infty$ since it falls off as $1/r^2$.

As $r \to 0$, I require that the radial probability density, $r^2|R_\ell(r)|^2 = |u_\ell(r)|^2$, be finite at the origin. Let us first consider $\ell \neq 0$ and assume the centrifugal potential term is larger than $V(r)$ as $r \to 0$. As $r \to 0$, the radial equation can then be approximated as

$$\frac{d^2u_\ell(r)}{dr^2} - \frac{\ell(\ell+1)}{r^2}u_\ell(r) = 0, \tag{10.38}$$

which has solutions $u_\ell(r) = r^{-\ell}, r^{\ell+1}$. The $r^{-\ell}$ solution must be rejected since it leads to a radial probability density that is not finite at the origin. Thus

$$u_\ell(r) \sim r^{\ell+1} \tag{10.39}$$

as $r \to 0$. This is a general result for any potential that rises or falls less quickly than $1/r^2$ as $r \to 0$. The power law dependence in Eq. (10.39) is not surprising; the larger the angular momentum, the further away from the origin we can expect to find the particle. The origin is a classically forbidden region if $\ell \neq 0$, since a classical particle having non-zero angular momentum cannot pass through the origin.

For $\ell = 0$, the situation must be examined on a case to case basis, using

$$\frac{d^2u_0(r)}{dr^2} + \frac{2\mu}{\hbar^2}[E - V(r)]u_0(r) = 0. \tag{10.40}$$

For attractive potentials that fall off faster than $-1/r^2$ there is no solution of the radial equation that satisfies the necessary boundary condition as $r \to 0$ when $\ell = 0$. In fact, for attractive potentials that fall off faster than $-1/r^2$ as $r \to 0$, there is no normalizable solution for any value of ℓ. For attractive potentials that fall off more slowly than $1/r^2$ as $r \to 0$, it would seem that the requirement that $|u_0(r)|^2$ be finite at the origin would not rule out the possibility that $R_0(r)$ varies as $1/r$, since $r^2 |R_0(r)|^2$ would then be finite; however, $\psi(\mathbf{r}) \sim 1/r$ is *not* a solution of Schrödinger's equation since, in that limit, the $\nabla^2 \psi(\mathbf{r})$ term in the Hamiltonian would give rise to a delta function that is not present in the potential. Therefore, as $r \to 0$, we must require that

$$u_0(r) = rR_0(r) \sim 0 \text{ as } r \to 0. \tag{10.41}$$

Generally speaking, for the potentials that I consider, the radial wave function $u_\ell(r)$ satisfies the boundary condition

$$u_\ell(r) = rR_\ell(r) \sim r^{\ell+1} \text{ as } r \to 0 \tag{10.42}$$

for *all* values of ℓ. In other words, $R_\ell(r)$ is finite at the origin.

To summarize, in bound state problem and for $\ell \neq 0$, there is a classically forbidden region that extends from $r = 0$ to $r_{\min}$, a classically allowed region between $r_{\min}$ and $r_{\max}$, and another classically forbidden region for $r > r_{\max}$ (recall that $r_{\min}$ and $r_{\max}$ are the turning points of the classical orbits for a given energy). For each value of ℓ, the lowest energy state radial wave function will have zero nodes in the classically allowed region, the next higher states, one node, etc. We can expect the radial wave function to have a polynomial or sinusoidal-like dependence in the classically allowed region. In the classically forbidden regions, the radial wave function has no nodes and $R_{E\ell}(r)$ approaches zero as $r \to 0$ (for $\ell \neq 0$) as r^ℓ and as some exponential power of r as $r \to \infty$. Each state having angular momentum quantum number ℓ is $(2\ell + 1)$ fold degenerate, owing to the spherical symmetry.

I now analyze the infinite spherical potential well, finite spherical potential well, Coulomb, and isotropic oscillator potentials.

10.3 Infinite Spherical Well Potential

The infinite spherical well potential is

$$V(r) = \begin{cases} 0 & r < a \\ \infty & r > a \end{cases}. \tag{10.43}$$

The effective potential in units of $\hbar^2/2\mu a^2$, with $L^2 = \hbar^2 \ell(\ell + 1)$, is shown in Fig. 10.2 as a function of r/a. Classically, there are bound states for any value of L

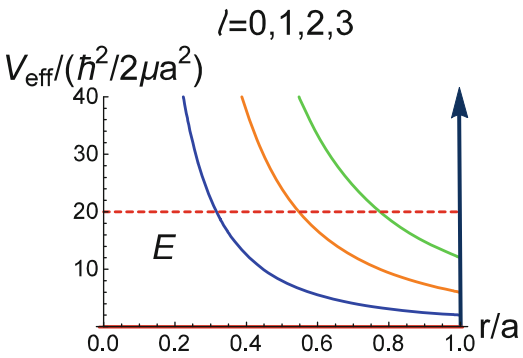

Fig. 10.2 Effective potential (in units of $\hbar^2/2\mu a^2$) for an infinite spherical well as a function of r/a. Curves corresponding to several values of angular momentum $L = \hbar\sqrt{\ell\,(\ell+1)}$ are shown (the $\ell = 0$ curve is along the horizontal axis). For each value of angular momentum, there is an infinity of discrete energies E possible classically. In the quantum problem, the energies are discrete. In both the classical and quantum cases, there is no upper bound to the allowed energies

and, for a given value of L, bound states occur for *all* energies

$$E \geq \frac{L^2}{2\mu a^2}, \tag{10.44}$$

where μ is the mass of the particle moving in the potential. In the quantum problem, you will see that the minimum energy for a given value of L is larger than that predicted by Eq. (10.44). Moreover the allowed energies are quantized rather than continuous. Classically, the particle is reflected each time it bounces off the spherical potential wall at $r = a$, but moves with constant velocity between bounces. There are no simple closed orbits, except for $L = 0$, when the particle moves along a diameter.

To introduce the quantum problem, let me first consider $\ell = 0$. The effective potential for $L = 0$ looks similar to that of the one-dimensional infinite square well potential (except, in the one-dimensional problem, the well width would be $2a$, going from $-a$ to a), but there is an important difference. In the three-dimensional problem, even though the potential vanishes at the center of the well, $r = 0$, there is a boundary condition that must be satisfied there. The boundary condition at $r = 0$ is $u_{k,\ell=0}(r) \equiv u_{k,0}(r) \sim r$, implying that $u_{k,0}(0) = 0$. In other words, solutions corresponding to even parity solutions of the analogous one-dimensional problem (which do not vanish at the center of the well) cannot occur in the three-dimensional case. *Remember*, the radial coordinate is *always* positive.

The solution for $\ell = 0$ is pretty simple. Equation (10.37) for the radial wave function when $r < a$ is

$$\frac{d^2u_{k,0}(r)}{dr^2} + k^2u_{k,0}(r) = 0, \tag{10.45}$$

where

$$k = \frac{\sqrt{2\mu E}}{\hbar}. \tag{10.46}$$

Solutions of this equation are sines and cosines of kr, but only the sine functions vanish at the origin, as required. Moreover, for the wave function to vanish at $r = a$,

$$k \to k_{n,\ell=0} \equiv k_{n0} = \frac{n\pi}{a}; \quad n = 1, 2, 3, \ldots, \tag{10.47a}$$

implying that the energy levels are quantized,

$$E_{n,\ell=0} = \frac{\hbar^2 k_{n0}^2}{2\mu}. \tag{10.47b}$$

The radial eigenfunctions are

$$R_{n0}(r) = \frac{u_{n0}(r)}{r} = \begin{cases} A\frac{\sin\left(\frac{n\pi r}{a}\right)}{r} & r < a \\ 0 & r \geq a \end{cases}, \tag{10.48}$$

where A is a normalization constant that is calculated below.

The *radial probability distribution* $P_{n\ell}(r)$ is obtained by looking at the probability to find the particle in a spherical shell between r and $r + dr$, namely

$$P_{n\ell}(r) = r^2 \int d\Omega \, |\psi_{n\ell}(\mathbf{r})|^2 = r^2 \, |R_{E\ell}(r)|^2 \int d\Omega \left|Y_\ell^m(\theta, \phi)\right|^2 = |u_{n\ell}(r)|^2 . \tag{10.49}$$

[For $\ell \neq 0$, I can still label the eigenfunctions by n, although the energy is no longer given by Eqs. (10.46) and (10.47a).] For $\ell = 0$,

$$\begin{aligned} P_{n0}(r) = |u_{n0}(r)|^2 &= \begin{cases} A^2 \sin^2\left(\frac{n\pi r}{a}\right) & r < a \\ 0 & r \geq a \end{cases} \\ &= \begin{cases} \frac{2}{a} \sin^2\left(\frac{n\pi r}{a}\right) & r < a \\ 0 & r \geq a \end{cases}, \end{aligned} \tag{10.50a}$$

where the value of A was obtained using the normalization condition

$$\int_0^\infty dr P_{n0}(r) = A^2 \int_0^a dr \sin^2\left(\frac{n\pi r}{a}\right) = 1. \tag{10.50b}$$

You can view the radial probability distribution as corresponding to the *odd parity eigenstates* of the one-dimensional problem for a well of size $2a$ located between $x = -a$ and $x = a$, provided you restrict the solution to $x > 0$.

Having considered the solution for $\ell = 0$, I now discuss the solution when $\ell \neq 0$. For each value of $\ell \neq 0$, there is an infinity of quantized energy levels with some minimum energy. It might be surprising, but, for $\ell \neq 0$, it is simpler to write the equation for $r < a$ in terms of $R_{k\ell}(r)$ instead of $u_{k\ell}(r)$, since the resulting equation

$$\frac{d^2R_{k\ell}(r)}{dr^2} + \frac{2}{r}\frac{dR_{k\ell}(r)}{dr} + \left[k^2 - \frac{\ell\,(\ell+1)}{r^2}\right]R_{k\ell}(r) = 0 \tag{10.51}$$

is recognized as a form of Bessel's equation. The independent solutions are the so-called *spherical Bessel and Neumann functions*,

$$j_\ell(x) = \sqrt{\frac{\pi}{2x}}J_{\ell+1/2}(x); \tag{10.52a}$$

$$n_\ell(x) = \sqrt{\frac{\pi}{2x}}N_{\ell+1/2}(x), \tag{10.52b}$$

where $J_\ell(x)$ and $N_\ell(x)$ are ordinary Bessel and Neumann functions. The Bessel functions $J_n(x)$ = BesselJ[n,x] and $N_n(x)$ = BesselY[n,x] are built in functions of *Mathematica,* as are the spherical Bessel functions $j_n(x)$ = SphericalBesselJ[n,x] and $n_n(x)$ = SphericalBesselY[n,x]. The general solution of the radial equation for $r < a$ is then

$$R_{k\ell}(r) = \frac{u_{k\ell}(r)}{r} = A_\ell j_\ell(kr) + B_\ell n_\ell(kr), \tag{10.53}$$

where A_ℓ and B_ℓ are constants (that also depend implicitly of k). The solution must be consistent with the boundary condition that $R_{k\ell}(r)$ be finite at the origin. As $x \to 0$

$$j_\ell(x) \sim \frac{x^{\ell+1}}{(2\ell+1)!!}; \tag{10.54a}$$

$$n_\ell(x) \sim \begin{cases} -\frac{1}{x} & \ell = 0 \\ -\frac{(2\ell-1)!!}{x^{\ell+1}} & \ell \neq 0 \end{cases}, \tag{10.54b}$$

where

$$(2\ell+1)!! = (1)\,(3)\ldots(2\ell-1)\,(2\ell+1)\,;$$

therefore, I must set $B_\ell = 0$ in Eq. (10.53) for all ℓ to satisfy the boundary at the origin. As a consequence, the radial wave functions are

$$R_{k\ell}(r) = \frac{u_{k\ell}(r)}{r} = \begin{cases} A_\ell j_\ell(kr) & r < a \\ 0 & r \geq a \end{cases}. \tag{10.55}$$

The first few spherical Bessel and Neumann functions are:

$$j_0(x) = \frac{\sin x}{x}; \tag{10.56a}$$

$$j_1(x) = \frac{\sin x}{x^2} - \frac{\cos x}{x}; \tag{10.56b}$$

$$j_2(x) = \left(\frac{3}{x^3} - \frac{1}{x}\right)\sin x - 3\frac{\cos x}{x^2}; \tag{10.56c}$$

$$n_0(x) = -\frac{\cos x}{x}; \tag{10.56d}$$

$$n_1(x) = -\frac{\cos x}{x^2} - \frac{\sin x}{x}; \tag{10.56e}$$

$$n_2(x) = -\left(\frac{3}{x^3} - \frac{1}{x}\right)\cos x - 3\frac{\sin x}{x^2}, \tag{10.56f}$$

and a useful asymptotic limit is

$$j_\ell(x) \sim \frac{\sin\left(x - \frac{\ell\pi}{2}\right)}{x}; \tag{10.57}$$

$$n_\ell(x) \sim \frac{-\cos\left(x - \frac{\ell\pi}{2}\right)}{x}, \tag{10.58}$$

valid for $x \gg 1$ and $x \gg \ell$.

Returning to the solution (10.55) and imposing the boundary condition that $R_{k\ell}(a) = 0$, I find

$$j_l(ka) = 0. \tag{10.59}$$

This equation can be solved numerically. For each ℓ, there is an associated effective potential that has an infinite number of energy levels. That is, for a given ℓ, the discrete energy levels can be labeled by

$$z_{n\ell} = k_{n\ell}a, \tag{10.60}$$

where $z_{n\ell}$ is the nth zero of the ℓth spherical Bessel function ($n = 1, 2, 3, \ldots$). For example, with $\ell = 1$, the lowest energy state has $z_{11} = (ka)_{11} \approx 4.5$, implying that

$$E_{11} = \frac{\hbar^2 k_{11}^2}{2\mu} = \frac{\hbar^2 k_{11}^2 a^2}{2\mu a^2} \approx 20.25\frac{\hbar^2}{2\mu a^2}. \tag{10.61}$$

The difference between the ground state energy for a given ℓ and the corresponding *classical* minimum energy $\left[\hbar^2\ell\left(\ell+1\right)/2\mu a^2\right]$, measured in units of $\hbar^2/2\mu a^2$ is equal to

$$\left(E_{1\ell} - E_\ell^{\text{class}}\right) / \left(\hbar^2/2\mu a^2\right) = \left(z_{1\ell}\right)^2 - \ell\left(\ell+1\right), \tag{10.62}$$

which is equal to π^2, 18.2, 27.2, 36.8 for $\ell = 0, 1, 2, 3$. The difference grows with increasing ℓ since Δr decreases with increasing ℓ (see Fig. 10.2), leading to larger values of Δp_r. As in the one-dimensional well, the energy levels for a given ℓ increase roughly as n^2 for large n, where n labels the corresponding zero of the spherical Bessel function.

The radial eigenfunctions are

$$R_{n\ell}(r) = \begin{cases} A_{n\ell} j_\ell(k_{n\ell} r) & r < a \\ 0 & r \geq a \end{cases} \tag{10.63}$$

and the radial probability distributions are

$$P_{n\ell}(r) = r^2 A_{n\ell}^2 j_\ell^2(k_{n\ell} r), \tag{10.64}$$

where the normalization coefficient is determined from

$$A_{n\ell} = \left[\int_0^a dr\, r^2 j_\ell^2(k_{n\ell} r) \right]^{-1/2}. \tag{10.65}$$

For each value of ℓ, the radial probability distribution has no node (other than that at $r = 0$ and $r = a$) for the lowest lying energy state, one node for the next higher energy state, etc. The dimensionless radial probability distribution $aP_{n\ell}(r)$ is plotted in Figs. 10.3, 10.4, and 10.5 as a function of r/a for $\ell = 0$, 5, 10 and $n = 1$, 2, 3. As you can see, the probability distribution is pushed further away from the origin with increasing ℓ, as would be expected from the effective potential shown in Fig. 10.2.

The classical radial probability distribution, obtained from Eqs. (10.6) and (10.7), is

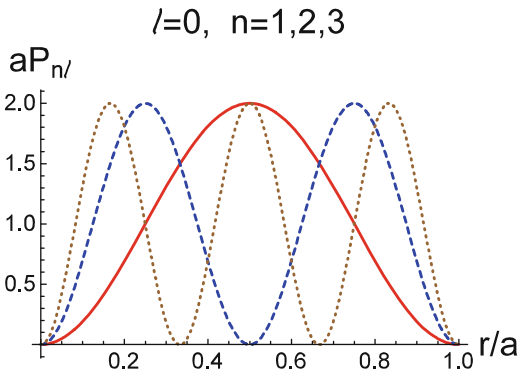

Fig. 10.3 Dimensionless radial probability distribution $aP_{n\ell}$ for the infinite well potential for $\ell = 0$ and $n = 1$ (red, solid), $n = 2$ (blue, dashed) and $n = 3$ (brown, dotted)

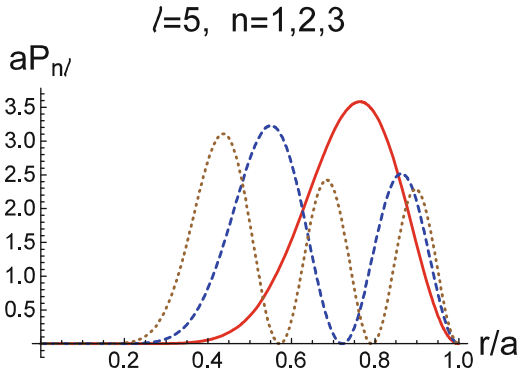

Fig. 10.4 Dimensionless radial probability distribution $aP_{n\ell}$ for the infinite well potential for $\ell = 5$ and $n = 1$ (red, solid), $n = 2$ (blue, dashed) and $n = 3$ (brown, dotted)

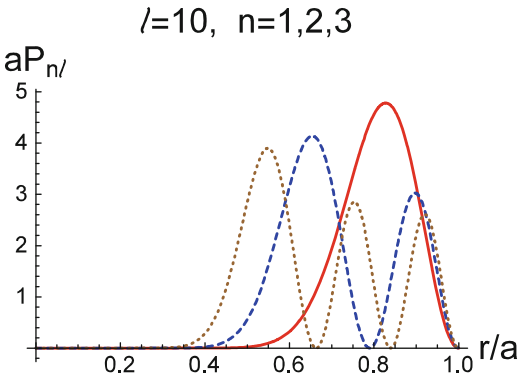

Fig. 10.5 Dimensionless radial probability distribution $aP_{n\ell}$ for the infinite well potential for $\ell = 10$ and $n = 1$ (red, solid), $n = 2$ (blue, dashed) and $n = 3$ (brown, dotted)

$$aP_{n\ell}^{\text{class}}(r) = \frac{z_{n\ell}}{\sqrt{\left(z_{n\ell}^2 - \frac{\ell(\ell+1)a^2}{r^2}\right)}\sqrt{\left(1 - \frac{\ell(\ell+1)}{z_{n\ell}^2}\right)}}. \tag{10.66}$$

To arrive at this result, I set

$$E = \frac{\hbar^2 k_{n\ell}^2}{2\mu}, \tag{10.67a}$$

$$L^2 = \hbar^2 \ell\,(\ell+1)\,, \tag{10.67b}$$

in Eqs. (10.6) and (10.7) to make a correspondence with the quantum problem and used $r_{\min} = a\sqrt{\ell\,(\ell+1)}/z_{n\ell}$ and $r_{\max} = a$ in carrying out the integral appearing in Eq. (10.6). In Fig. 10.6, I plot $aP_{n\ell}(r)$ as a function of r/a for $\ell = 5$ and $n = 10$, along with the classical probability distribution. As you can see, the quantum radial

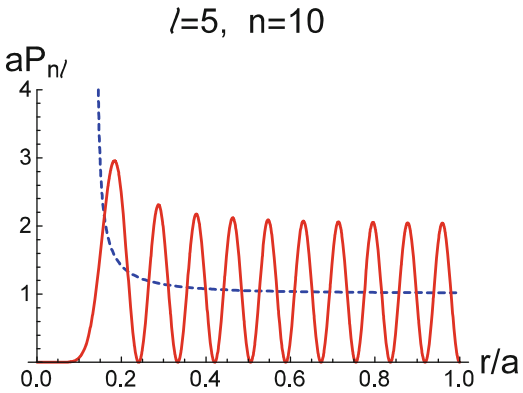

Fig. 10.6 Dimensionless radial probability distribution $aP_{n\ell}$ for the infinite well potential for $\ell = 5$ and $n = 10$; quantum distribution (red, solid), classical distribution (blue, dashed)

probability distribution in the classically allowed region, averaged over oscillations, is in good agreement with the classical distribution. The classically allowed region, obtained by solving Eq. (10.7), is defined by

$$\sqrt{\ell\,(\ell+1)}/z_{n\ell} < r/a < 1. \tag{10.68}$$

For $\ell = 5$ and $n = 10$, I find that $z_{10,5} = 38.9$ and that the classically allowed region is $0.141 < r/a < 1$.

Before leaving this section, I would like to return to the case of $\ell = 0$, for which

$$P_{n0}(r) = \begin{cases} \frac{2}{a}\sin^2\left(\frac{n\pi r}{a}\right) & r < a \\ 0 & r \geq a \end{cases}.$$

For large n, the radial probability density oscillates rapidly. When averaged over these oscillations, the radial probability distribution reduces to $\overline{P_{n0}(r)} = 1/a$, the *classical* probability distribution for a free particle moving along a diameter of the well. In the classical problem, the particle moves along a specific diameter (depending on the initial conditions), but in the quantum problem $|\psi_{E\ell m}(\mathbf{r})|^2 = \left|R_{E\ell}(r)Y_0^0(\theta,\phi)\right|^2 = R_{E\ell}^2(r)/4\pi$ is *spherically symmetric*. Remember that in the classical limit, quantum probability distributions correspond to classical distributions, *averaged over all possible initial conditions*. If we average the classical result over all possible initial conditions when $L = 0$, there cannot be any θ dependence since motion along every diameter of the sphere is equally likely.

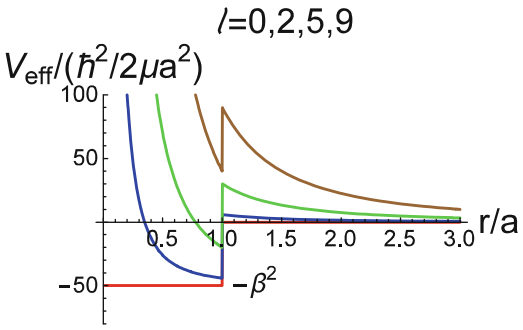

Fig. 10.7 Effective potential (in units of $\hbar^2/2\mu a^2$) for a finite spherical well as a function of r/a for $\beta^2 = 50$. Curves corresponding to several values of angular momentum $L = \hbar\sqrt{\ell\,(\ell+1)}$ are shown

10.4 Finite Spherical Well Potential: Bound States

Next I consider the spherical well potential,

$$V(r) = \begin{cases} -V_0 < 0 & r < a \\ 0 & r > a \end{cases}. \tag{10.69}$$

I consider only bound states, that is states for which $E < 0$. The effective potential in units of $\hbar^2/2\mu a^2$, with $L^2 = \hbar^2\ell\,(\ell+1)$, is shown in Fig. 10.7 as a function of r/a for $\ell = 0, 2, 5, 9$. Note that the value of V_0 in these units is β^2 (that is, $V_0/\left(\hbar^2/2\mu a^2\right) = \beta^2$). It is clear from the figure that, for fixed V_0, the number of bound states decreases with increasing angular momentum. A necessary (but not sufficient) condition for bound states to exist is

$$\ell\,(\ell+1) < \frac{2\mu V_0}{\hbar^2}a^2 = \beta^2; \tag{10.70}$$

otherwise, the effective potential is everywhere positive and E must be positive as well. When condition (10.70) is satisfied, the number of bound states, *if any*, depends on the values of ℓ and β.

The radial equation for $r < a$ is

$$\frac{d^2R_{E\ell}(r)}{dr^2} + \frac{2}{r}\frac{dR_{E\ell}(r)}{dr} + \left[k'^2 - \frac{\ell\,(\ell+1)}{r^2}\right]R_{E\ell}(r) = 0, \tag{10.71}$$

where

$$k' = \frac{\sqrt{2\mu\,(E+V_0)}}{\hbar} > 0, \tag{10.72}$$

while, for $r > a$, the equation is

$$\frac{d^2R_{E\ell}(r)}{dr^2} + \frac{2}{r}\frac{dR_{E\ell}(r)}{dr} + \left[-\kappa^2 - \frac{\ell\,(\ell+1)}{r^2}\right]R_{E\ell}(r) = 0, \tag{10.73}$$

where

$$\kappa = \frac{\sqrt{-2\mu E}}{\hbar} > 0. \tag{10.74}$$

In both cases, the equation is a form of Bessel's equation, but I must chose the appropriate solutions consistent with the boundary conditions. The radial wave function must be finite at the origin and must not blow up as $r \to \infty$. To satisfy these boundary conditions, I take

$$R_{E\ell}(r) = \begin{cases} A_\ell j_l(k'r) & r < a \\ B_\ell h_l^{(1)}(i\kappa r) & r > a \end{cases}, \tag{10.75}$$

where

$$h_l^{(1)}(z) = j_l(z) + in_\ell(z) \tag{10.76}$$

is a *spherical Hankel function of the first kind* for which $h_l^{(1)}(i\kappa r) \sim e^{-\kappa r}$ as $r \to \infty$. The eigenenergies can then be obtained by equating the radial wave function and its derivative at $r = a$, and then solving the resulting equations graphically. In other words, I set

$$A_\ell j_l(k'a) = B_\ell h_l^{(1)}(i\kappa a); \tag{10.77a}$$

$$k'A_\ell j_l'(k'a) = i\kappa B_\ell h_l'^{(1)}(i\kappa a), \tag{10.77b}$$

where the primes on the Bessel or Hankel functions indicate derivatives that are a shorthand notation for

$$j_l'(k'a) = \left.\frac{dj_l(z)}{dz}\right|_{z=k'a} \tag{10.78a}$$

$$h_l^{(1)\prime}(i\kappa a) = \left.\frac{dh_l^{(1)}(z)}{dz}\right|_{z=i\kappa a}. \tag{10.78b}$$

Dividing Eqs. (10.77), I find

$$\frac{j_l(k'a)}{k'j_l'(k'a)} = \frac{h_l^{(1)}(i\kappa a)}{i\kappa h_l^{(1)\prime}(i\kappa a)}. \tag{10.79}$$

If you use the fact that $(k'a)^2 = \beta^2 - (\kappa a)^2$, where β is defined by Eq. (10.70), you can solve Eq. (10.79) graphically for (κa) for each value of ℓ and β. The solution determines the energy (see problems).[1]

For $\ell = 0$, I can use the fact that

$$j_0(z) = \frac{\sin z}{z}; \quad h_0^{(1)}(z) = -i\frac{e^{iz}}{z} \tag{10.80}$$

to evaluate Eq. (10.79), but it is easiest to return directly to Eq. (10.37),

$$\frac{d^2u_{E,0}(r)}{dr^2} + k'^2 u_{E,0}(r) = 0 \tag{10.81}$$

for $r < a$ and

$$\frac{d^2u_{E,0}(r)}{dr^2} - \kappa^2 u_{E,0}(r) = 0 \tag{10.82}$$

for $r > a$. The appropriate solutions of these equations are

$$u_{E,\ell=0}(r) = \begin{cases} A_0 \sin(k'r) & r < a \\ B_0 \exp(-\kappa r) & r > a \end{cases} \tag{10.83}$$

(only the sin solution can be taken for $r < a$ since $R_0(r) = u_0(r)/r$ must be regular at the origin). You can now solve as we did for a potential well in one dimension having width $2a$, although the solution corresponds only to the *odd* parity solutions of that problem since $u_{E,0}$ must vanish at $r = 0$, and only to the region $x > 0$ since r must be positive. There is a bound state for $\ell = 0$ only if $\beta > \pi/2$.

For values of $\ell \geq 1$, there are correspondingly higher values of β needed to support a bound state. The actual values for the eigenenergies and the number of allowed solutions are obtained by solving Eq. (10.79). For sufficiently large ℓ that violate condition (10.70), no bound states can exist in the quantum problem, even though positive energy, *classical* bound states can always be found for the effective potentials shown in Fig. 9.8 for any value of ℓ.

10.5 Bound State Coulomb Problem (Hydrogen Atom)

The electrostatic Coulomb potential is

$$V(r) = -\frac{K_e}{r}, \tag{10.84}$$

[1]The function $h_l^{(1)}(i\kappa a)$ is real for even ℓ and purely imaginary for odd ℓ, while the function $h_l'^{(1)}(i\kappa a)$ is real for odd ℓ and purely imaginary for even ℓ; as a consequence, the right-hand side of Eq. (10.79) is always real.

where $K_e = e^2/4\pi\epsilon_0$ is a constant. For hydrogen, the mass that appears in the Hamiltonian is not the electron mass m, but the reduced mass $\mu = mm_p/\left(m + m_p\right)$ where m_p is the proton mass. The radius r appearing in Eq. (10.84) is then the relative electron–proton separation. The effective potential is shown in Fig. 10.1; classical bound states are possible for a range of negative energies, independent of the value of ℓ. Looking at the effective potentials in Fig. 10.1, you might think that, for large ℓ, the wells are too shallow to support a bound state in the quantum problem. It turns out, however, that this is *not* the case. The slow fall off of a $1/r$ potential leads to a situation where, for any value of ℓ, there is an infinite number of bound states. For the classical problem, there is a continuum of bound state energies for each L, while in the quantum problem there is a discrete infinity of bound state energies for each ℓ.

For the potential of Eq. (10.84), the radial equation, Eq. (10.37), reduces to

$$\frac{d^2u_\ell(r)}{dr^2} + \frac{2\mu}{\hbar^2}\left[E + \frac{K_e}{r} - \frac{\hbar^2\ell\left(\ell+1\right)}{2\mu r^2}\right]u_\ell(r) = 0. \tag{10.85}$$

It is convenient to introduce dimensionless variables

$$\rho = r/a_0; \tag{10.86a}$$

$$\lambda = -E/E_R; \tag{10.86b}$$

$$u_\ell(r) \to v_\ell(\rho), \tag{10.86c}$$

where

$$a_0 = \frac{\hbar^2}{\mu K_e} = \frac{\hbar}{\mu c}\frac{1}{\alpha_{FS}} = 5.29\times10^{-11}\ \text{m}; \tag{10.87a}$$

$$E_R = \frac{1}{2}\frac{K_e}{a_0} = \frac{1}{2}\mu c^2\alpha_{FS}^2 = 13.6\ \text{eV}; \tag{10.87b}$$

$$\alpha_{FS} = \frac{K_e}{\hbar c} = \frac{1}{4\pi\epsilon_0}\frac{e^2}{\hbar c} \approx \frac{1}{137}. \tag{10.87c}$$

In terms of these variables, Eq. (10.85) is transformed into

$$\frac{d^2v_\ell(\rho)}{d\rho^2} + \left[-\lambda + \frac{2}{\rho} - \frac{\ell\left(\ell+1\right)}{\rho^2}\right]v_\ell(\rho) = 0. \tag{10.88}$$

This is a somewhat general dimensionless form of the radial equation. For different potentials the only term that changes is the $2/\rho$ term. I can build in the asymptotic dependence of the radial wave functions as $\rho \to 0$ and as $\rho \to \infty$. The boundary condition as $\rho \to 0$ is

$$v_\ell(\rho) \sim \rho^{\ell+1}. \tag{10.89}$$

As $\rho \to \infty$, the radial equation can be approximated as

$$\frac{d^2 v_\ell(\rho)}{d\rho^2} - \lambda v_\ell(\rho) = 0 \tag{10.90}$$

which has solutions $v_\ell(\rho) = e^{\pm\sqrt{\lambda}\rho}$. The $e^{\sqrt{\lambda}\rho}$ solution must be rejected since it leads to a radial wave function that blows up as $\rho \to \infty$. Thus

$$v_\ell(\rho) \sim e^{-\sqrt{\lambda}\rho} \tag{10.91}$$

as $\rho \to \infty$. This is a general result for the radial equation for any potential that goes to zero as $\rho \to \infty$. The exponential dependence is not surprising since the particle must penetrate into the classically forbidden.

Building in both asymptotic limits, I try a solution of the form

$$v_\ell(\rho) = \rho^{\ell+1} e^{-\sqrt{\lambda}\rho} f_\ell(\rho), \tag{10.92}$$

calculate

$$\begin{aligned} v_\ell''(\rho) = {} & \ell\,(\ell+1)\,\rho^{\ell-1} e^{-\sqrt{\lambda}\rho} f_\ell(\rho) \\ & -2\sqrt{\lambda}\,(\ell+1)\,\rho^{\ell} e^{-\sqrt{\lambda}\rho} f_\ell(\rho) - 2\sqrt{\lambda}\rho^{\ell+1} e^{-\sqrt{\lambda}\rho} f_\ell'(\rho) \\ & +2\,(\ell+1)\,\rho^{\ell} e^{-\sqrt{\lambda}\rho} f_\ell'(\rho) + \rho^{\ell+1} e^{-\sqrt{\lambda}\rho} f_\ell''(\rho) \\ & +\lambda\rho^{\ell+1} e^{-\sqrt{\lambda}\rho} f_\ell(\rho), \end{aligned} \tag{10.93}$$

and substitute the result into Eq. (10.88) to arrive at

$$\rho f_\ell''(\rho) + 2\left[(\ell+1) - \rho\sqrt{\lambda}\right] f_\ell'(\rho) + 2\left[1 - (\ell+1)\sqrt{\lambda}\right] f_\ell(\rho) = 0. \tag{10.94}$$

I now make two additional changes of variable,

$$y = 2\rho\sqrt{\lambda}; \tag{10.95a}$$

$$f_\ell(\rho) \to g_\ell(y), \tag{10.95b}$$

which transforms Eq. (10.94) into

$$y\frac{d^2 g_\ell}{dy^2} + (\alpha + 1 - y)\frac{dg_\ell}{dy} + \left[\frac{1}{\sqrt{\lambda}} - (\ell+1)\right] g_\ell = 0, \tag{10.96}$$

where

$$\alpha = 2\ell + 1. \tag{10.97}$$

Equation (10.96) is known as *Laguerre's differential equation*. Only if $\alpha > -1$ do solutions of this equation exist that are regular as $\rho \to \infty$. This condition on α is a necessary but not sufficient condition for regular solutions to exist as $\rho \to \infty$. In addition it is necessary that

$$\frac{1}{\sqrt{\lambda}} - (\ell + 1) = q, \tag{10.98}$$

where q is a positive integer or zero. When both these conditions are satisfied, the physically acceptable solutions of Eq. (10.96) are

$$g_{\alpha\lambda}(y) = L_q^\alpha(y). \tag{10.99}$$

The $L_q^\alpha(y)$ are the *generalized Laguerre polynomials* that satisfy the differential equation

$$y\frac{d^2L_q^\alpha(y)}{dy^2} + (\alpha + 1 - y)\frac{dL_q^\alpha(y)}{dy} + qL_q^\alpha(y) = 0. \tag{10.100}$$

Some properties of the generalized Laguerre polynomials [*Mathematica* symbol LaguerreL$[q, \alpha, y] = L_q^\alpha(y)$] are listed in the Appendix.

For the hydrogen atom problem,

$$\alpha = 2\ell + 1 > -1; \tag{10.101a}$$

$$q = \frac{1}{\sqrt{\lambda}} - (\ell + 1)\,. \tag{10.101b}$$

The requirement that q be a non-negative integer leads us to the condition

$$\frac{1}{\sqrt{\lambda}} = q + \ell + 1 = n, \tag{10.102}$$

where n is defined as $(q + \ell + 1)$. From Eq. (10.102) and the fact that both q and ℓ are non-negative integers, it follows that

$$n \geq 1 \quad \text{and} \quad \ell \leq n - 1. \tag{10.103}$$

As was to be expected from classical considerations, there is a maximum angular momentum for a fixed energy.

The eigenenergies are given by

$$E_n = -\lambda E_R = -\frac{1}{2}\frac{\mu c^2 \alpha_{FS}^2}{n^2}; \qquad n = 1, 2, 3, \ldots. \tag{10.104}$$

For each value of n, ℓ can equal $0, 1, \ldots, (n-1)$, and, for each value of ℓ, m can equal $0, \pm 1, \pm 2, \ldots \pm \ell$. Thus, the energy degeneracy for a given n is

$$\sum_{\ell=0}^{n-1} (2\ell + 1) = n^2. \tag{10.105}$$

There is an "accidental degeneracy" for states having the same n, but different ℓ. This can be related to the fact that there is a conserved *dynamic* constant called the Lenz vector that points in the direction of the semi-major axis of the classical problem (the orbits are closed). In group theory the symmetry is related to the group O(4), the orthogonal group in four dimensions.

The solution of Eq. (10.96) is

$$g_{\alpha q}(y) = L_q^{\alpha}(y) = L_{n-\ell-1}^{2\ell+1}\left(2\rho\sqrt{\lambda}\right) = L_{n-\ell-1}^{2\ell+1}\left(\frac{2\rho}{n}\right). \tag{10.106}$$

To get the total radial wave function $R_{n\ell}(\rho) \sim v_\ell(\rho)/\rho$, I must multiply $L_{n-\ell-1}^{2\ell+1}\left(\frac{2\rho}{n}\right)$ by $\rho^\ell e^{-\rho/n}$ [see Eq. (10.92)]. The normalized dimensionless wave function can then be written as

$$\tilde{\psi}_{n\ell m}(\boldsymbol{\rho}) = \tilde{R}_{n\ell}(\rho) Y_\ell^m(\theta, \phi), \tag{10.107}$$

where the dimensionless radial wave function $\tilde{R}_{n\ell}(\rho)$ is

$$\begin{aligned} \tilde{R}_{n\ell}(\rho) &= \left(\frac{2}{\rho n^3}\right)^{1/2} \Lambda_{n-\ell-1}^{2\ell+1}\left(\frac{2\rho}{n}\right) \\ &= \frac{2}{n^2}\sqrt{\frac{(n-\ell-1)!}{(n+\ell)!}}\left(\frac{2\rho}{n}\right)^\ell e^{-\rho/n} L_{n-\ell-1}^{2\ell+1}\left(\frac{2\rho}{n}\right), \end{aligned} \tag{10.108}$$

and

$$\Lambda_q^{2\ell+1}(\rho) = \sqrt{\frac{q!}{(q+2\ell+1)!}} e^{-\rho/2} \rho^{\ell+1/2} L_q^{2\ell+1}(\rho) \tag{10.109}$$

is an *associated Laguerre function*. The $\tilde{\psi}_{n\ell m}(\boldsymbol{\rho})$ constitute an orthonormal set.

From the Appendix, some properties of the $L_{n-\ell-1}^{2\ell+1}$ and $\Lambda_q^{2\ell+1}$ functions are

$$L_q^{2\ell+1}(\rho) \text{ is a polynomial of order } q; \tag{10.110a}$$

$$\int_0^\infty d\rho L_q^{2\ell+1}(\rho) L_{q'}^{2\ell+1}(\rho) e^{-\rho} \rho^{2\ell+1} = \frac{(q+2\ell+1)!}{q!} \delta_{q,q'}; \tag{10.110b}$$

$$\rho\Lambda_{n-\ell-1}^{2\ell+1}(\rho) = 2n\Lambda_{n-\ell-1}^{2\ell+1}(\rho) - \sqrt{(n+\ell+1)(n-\ell)}\Lambda_{n-\ell}^{2\ell+1}(\rho) - \sqrt{(n-\ell-1)(n+\ell)}\Lambda_{n-\ell-2}^{2\ell+1}(\rho); \tag{10.110c}$$

$$\int_0^\infty d\rho\Lambda_q^\alpha(\rho)\Lambda_{q'}^\alpha(\rho) = \delta_{q,q'}; \tag{10.110d}$$

$$2\left(\frac{1}{n^3n'^3}\right)^{1/2}\int_0^\infty d\rho\,\rho\Lambda_{n-\ell-1}^{2\ell+1}\left(\frac{2\rho}{n}\right)\Lambda_{n'-\ell-1}^{2\ell+1}\left(\frac{2\rho}{n'}\right) = \delta_{n,n'}. \tag{10.110e}$$

The number of nodes in the radial wave function is $q = n - \ell - 1$.

The first few dimensionless radial wave functions are

$$\tilde{R}_{10}(\rho) = 2e^{-\rho}; \tag{10.111a}$$

$$\tilde{R}_{20}(\rho) = \frac{(2-\rho)\,e^{-\rho/2}}{2\sqrt{2}}; \tag{10.111b}$$

$$\tilde{R}_{21}(\rho) = \frac{\rho e^{-\rho/2}}{2\sqrt{6}}; \tag{10.111c}$$

$$\tilde{R}_{30}(\rho) = \frac{2\left(27-18\rho+2\rho^2\right)e^{-\rho/3}}{81\sqrt{3}}; \tag{10.111d}$$

$$\tilde{R}_{31}(\rho) = \frac{4\,(6-\rho)\,\rho e^{-\rho/3}}{81\sqrt{6}}; \tag{10.111e}$$

$$\tilde{R}_{32}(\rho) = \frac{2}{81}\sqrt{\frac{2}{15}}\rho^2 e^{-\rho/3}. \tag{10.111f}$$

Dimensionless radial wave functions are plotted in Figs. 10.8, 10.9 and 10.10 for $n = 1, 2, 3$.

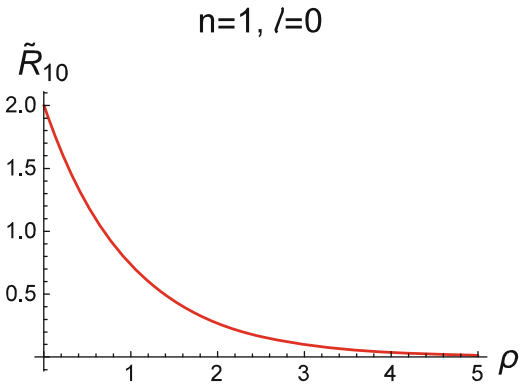

Fig. 10.8 Dimensionless hydrogenic radial wavefunction for $n = 1$

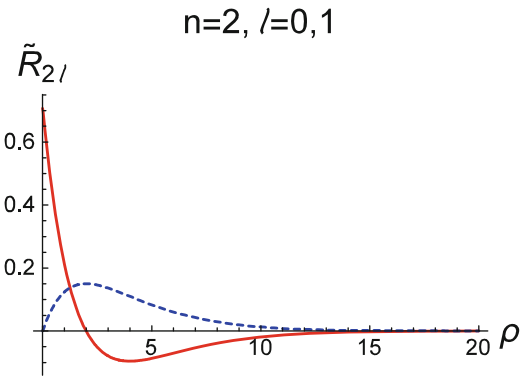

Fig. 10.9 Dimensionless hydrogenic radial wave function for $n = 2$. $\ell = 0$ (red, solid); $\ell = 1$ (blue, dashed)

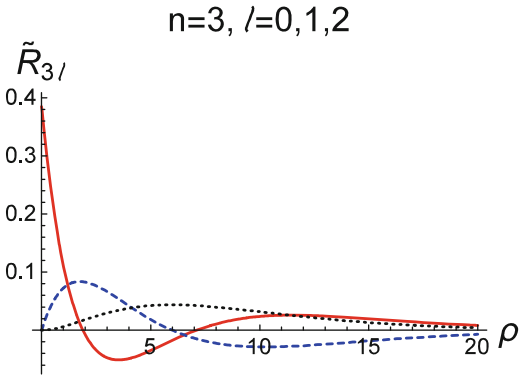

Fig. 10.10 Dimensionless hydrogenic radial wavefunction for $n = 3$. $\ell = 0$ (red, solid); $\ell = 1$ (blue, dashed); $\ell = 2$ (black, dotted)

Going from an eigenfunction that is dimensionless to one that has dimensions of $1/\sqrt{\text{volume}}$ is accomplished by taking

$$\psi_{n\ell m}(\mathbf{r}) = R_{n\ell}(r) Y_\ell^m(\theta, \phi)\,, \tag{10.112}$$

where the radial wave function is

$$R_{n\ell}(r) = \frac{1}{a_0^{3/2}} \tilde{R}_{n\ell}\left(\frac{r}{a_0}\right) \tag{10.113}$$

or

$$R_{n\ell}(r) = \frac{1}{a_0^{3/2}} \left(\frac{2}{n^2}\right) \sqrt{\frac{(n-\ell-1)!}{(n+\ell)!}} \left(\frac{2r}{na_0}\right)^\ell e^{-r/na_0} L_{n-\ell-1}^{2\ell+1}\left(\frac{2r}{na_0}\right). \tag{10.114}$$

In order to gain some physical insight into the radial dependence of the eigenfunctions, I calculate the radial probability distribution and compare it with the corresponding classical radial probability distribution. In dimensionless units, the quantum radial probability distribution is

$$\begin{aligned}\tilde{P}_{n\ell}(\rho) &= \rho^2 \tilde{R}^2_{n\ell}(\rho) = \left(\frac{2}{n^3}\right)\rho\left[\Lambda^{2\ell+1}_{n-\ell-1}(2\rho/n)\right]^2 \\ &= \left(\frac{1}{n^2}\right)\frac{(n-\ell-1)!}{(n+\ell)!}e^{-2\rho/n}\left(\frac{2\rho}{n}\right)^{2\ell+2} \\ &\quad\times\left[L^{2\ell+1}_{n-\ell-1}(2\rho/n)\right]^2. \end{aligned} \tag{10.115}$$

On the other hand, the classical radial probability distribution in dimensionless units, obtained using Eq. (10.6), is given by

$$\begin{aligned}\tilde{P}^{\text{class}}_{n\ell}(\rho) &= a_0 P^{\text{class}}(a_0\rho) \\ &= \frac{a_0}{T_{21}\sqrt{\frac{2K_e}{\mu a_0}}\sqrt{\left(-\frac{1}{2n^2}+\frac{1}{\rho}-\frac{\ell(\ell+1)}{2\rho^2}\right)}}, \end{aligned} \tag{10.116}$$

where a_0 is the Bohr radius and I have set $E = -E_R/n^2 = -K_e/\left(2n^2 a_0\right)$ and $L^2 = \hbar^2\ell\,(\ell+1)$. Equations (10.5) and (10.7) can be used to obtain

$$T_{21} = \pi\sqrt{-\frac{\mu K_e^2}{8E^3}} = \pi n^3\sqrt{\frac{\mu a_0^3}{K_e}}. \tag{10.117}$$

Note that T_{21} is one-half the period of the classical orbit. Combining Eqs. (10.116) and (10.117), I obtain the classical probability distribution

$$\tilde{P}^{\text{class}}_{n\ell}(\rho) = \frac{1}{\pi n^3\sqrt{-\frac{1}{n^2}+\frac{2}{\rho}-\frac{\ell(\ell+1)}{\rho^2}}}. \tag{10.118}$$

There are two turning points, given by

$$\rho_{\min,\max}(n,\ell) = n^2\left[1 \mp \sqrt{1-\frac{\ell\,(\ell+1)}{n^2}}\right]. \tag{10.119}$$

These classical turning points correspond to positions in the orbit when the electron is located along the semi-major axis of the ellipse. For fixed energy (fixed n) $\rho_{\min}(n,\ell)$ decreases and $\rho_{\max}(n,\ell)$ increases with decreasing ℓ, a result that is deduced easily from graphs of the effective potential. The value $\ell = n-1$ corresponds most closely to circular orbits; in this limit

$$\rho_{\min,\max}(n, n-1) = n^2\left[1 \mp \frac{1}{n}\right] \tag{10.120}$$

and the relative width of the distribution is

$$\frac{\rho_{\max}(n, n-1) - \rho_{\min}(n, n-1)}{\left[\rho_{\max}(n, n-1) + \rho_{\min}(n, n-1)\right]/2} = \frac{2n}{n^2} = \frac{2}{n}. \tag{10.121}$$

With increasing n, the classical distribution for $\ell = n-1$ corresponds more closely to circular orbits. Of course, circular orbits *are* possible in the classical case for an energy equal to the effective potential at its minimum; however, the values I chose to simulate the quantum variables, $E_n = -K_e/\left(2n^2 a_0\right)$ and $L^2 = \hbar^2 \ell\,(\ell+1)$, do not correspond to circular orbits.

I now return to the quantum probability distribution, Eq. (10.115). It possesses many of the features of the classical distribution function in the classically allowed region. For example, for $\ell = n-1$

$$\tilde{P}_{n,n-1}(\rho) = \frac{1}{n^2\,(2n-1)!}\left(\frac{2}{n}\right)^{2n} e^{-2\rho/n}\rho^{2n}. \tag{10.122}$$

This function possesses a single maximum at $\rho_c = n^2$ or $r_c = n^2 a_0$ and a relative width of order of that given by Eq. (10.121). For smaller values of ℓ, the orbits correspond to classical elliptical orbits and the electron spends less time when it is nearest to the proton, corresponding to the fact that the speed in the classical orbits is larger, the closer the electron is to the nucleus. There are $n-\ell-1$ nodes in the classically allowed region. Using the recursion relation (10.110c), you can show that

$$\langle\rho\rangle = \int_0^\infty \rho\tilde{P}_{n\ell}(\rho) = \frac{3n^2 - \ell\,(\ell+1)}{2}, \tag{10.123}$$

which is also equal to $\langle\rho\rangle$ for the classical probability distribution given by Eq. (10.118).

The (dimensionless) quantum radial probability distribution is plotted in Figs. 10.11, 10.12 and 10.13 as a function of ρ/n^2 for $n = 40$ and $\ell = 39, 25, 0$ as the solid red curves. For $\ell = n-1 = 39$ (which corresponds most closely to circular orbits), the maximum of occurs at $\rho/n^2 = 1$. For $\ell = 10$, you can see the relative maxima in the envelope of the distribution at the inner and outer turning points, $\rho_{\min,\max}(n,\ell)/n^2 = 0.23, 1.77$, with the probability largest at the outer turning point. For $\ell = 0$, the probability distribution extends to the center of force and the envelope has a single maximum near the classical turning point at $\rho/n^2 = 2$. The classical radial probability distribution $\tilde{P}^{\text{class}}_{n\ell}(\rho)$ is superimposed on the quantum distribution as the dashed blue curves in Figs. 10.11, 10.12 and 10.13. It is seen that it agrees very well with the quantum distribution, averaged over oscillations, in the classically allowed region.

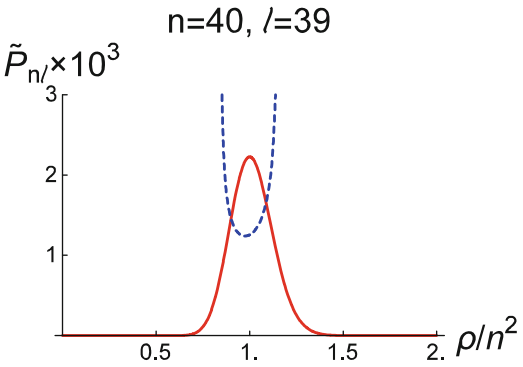

Fig. 10.11 Quantum (solid, red) and classical (blue, dashed) radial probability distributions for hydrogen for $n = 40$, $\ell = 39$

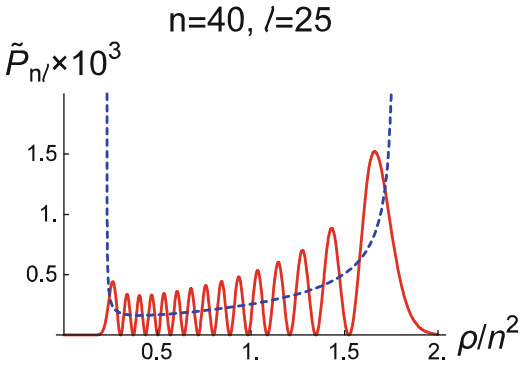

Fig. 10.12 Quantum (solid, red) and classical (blue, dashed) radial probability distributions for hydrogen for $n = 40$, $\ell = 25$

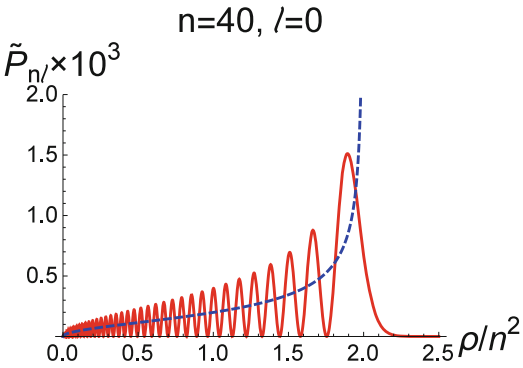

Fig. 10.13 Quantum (solid, red) and classical (blue, dashed) radial probability distributions for hydrogen for $n = 40$, $\ell = 0$

10.6 3-D Isotropic Harmonic Oscillator

The potential energy for an isotropic oscillator is

$$V(r) = \frac{1}{2}\mu\omega^2 r^2. \tag{10.124}$$

I have already solved this problem in rectangular coordinates [see Sect. 8.1.3]. The eigenenergies are

$$E_n = \left(n + \frac{3}{2}\right)\hbar\omega, \tag{10.125}$$

where n is a positive integer or zero. There is an $(n+1)(n+2)/2$ fold degeneracy for each value of n.

I can formulate a "Bohr theory" for circular orbits for the oscillator, in which

$$\mu v r = \mu\omega r^2 = (n+1)\hbar; \quad n = 0, 1, 2, \ldots. \tag{10.126}$$

$$F = \frac{\mu v^2}{r} = \mu\omega^2 r, \tag{10.127}$$

leading to

$$r_n = \sqrt{(n+1)}\sqrt{\frac{\hbar}{\mu\omega}}, \tag{10.128}$$

$$v_n = \sqrt{(n+1)}\sqrt{\frac{\hbar\omega}{\mu}}, \tag{10.129}$$

and

$$E_n = \hbar\omega\,(n+1)\,. \tag{10.130}$$

The energy spacing is correct, but the levels are displaced by $-\hbar\omega/2$ from the true values.

The effective potential in units of $\hbar\omega$ is shown in Fig. 10.14 as a function of $\xi = \sqrt{\mu\omega/\hbar}\,r$ for $\ell = 0, 2, 5, 9$. The effective potential for $\ell = 0$ is the same as that for the one-dimensional harmonic oscillator, restricted to $x > 0$. However, since the wave function must be finite at the origin, only the odd parity solutions of the one-dimensional oscillator are allowed. In other words, for $\ell = 0$, the energies are

$$E_{n,\ell=0} = (q + 1/2)\,\hbar\omega; \quad q = 1, 3, 5, \ldots \tag{10.131a}$$

$$= (n + 3/2)\,\hbar\omega; \quad n = 0, 2, 4, \ldots \tag{10.131b}$$

Thus, $\ell = 0$ states appear only in states with n *even*. This is not a surprise. The parity of the eigenstates, obtained from Eq. (8.18) is $(-1)^{n_x+n_y+n_z} = (-1)^n$. Since

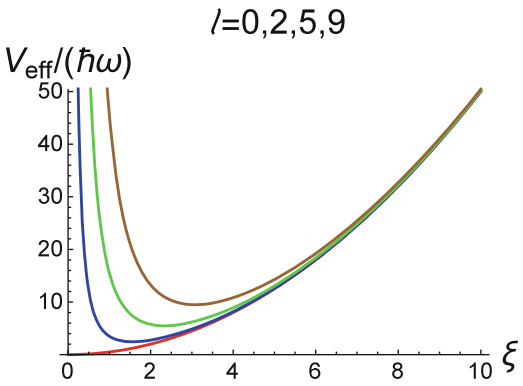

Fig. 10.14 Effective potential for the 3-D oscillator in units of $\hbar\omega$ as a function of $\xi = \sqrt{\mu\omega/\hbar}r$ for $\ell = 0, 2, 5, 9$

the parity of an $\ell = 0$ state is equal to $+1$, the value of n for all states having $\ell = 0$ must be even. As you shall see, for a given n, only those ℓ values are allowed for which $(-1)^\ell = (-1)^n$.

In spherical coordinates, the radial equation in terms of a dimensionless coordinate

$$\xi = \sqrt{\frac{\mu\omega}{\hbar}}r \tag{10.132}$$

and a dimensionless energy

$$\lambda = 2E/\hbar\omega \tag{10.133}$$

is

$$\frac{d^2u_{\lambda\ell}(\xi)}{d\xi^2} + \left[\lambda - \xi^2 - \frac{\ell\,(\ell+1)}{\xi^2}\right]u_{\lambda\ell}(\xi) = 0. \tag{10.134}$$

Assuming a solution of the form

$$u_{\lambda\ell}(\xi) = \xi^{\ell+1}e^{-\xi^2/2}f_{\lambda\ell}(\xi), \tag{10.135}$$

I calculate

$$\begin{aligned} u''_{\lambda\ell}(\xi) &= \ell\,(\ell+1)\,\xi^{\ell-1}e^{-\xi^2/2}f_{\lambda\ell}(\xi) \\ &\quad - (2\ell+3)\,\xi^{\ell+1}e^{-\xi^2/2}f_{\lambda\ell}(\xi) - 2\xi^{\ell+2}e^{-\xi^2/2}f'_{\lambda\ell}(\xi) \end{aligned}$$

$$+2(\ell+1)\xi^{\ell}e^{-\xi^2/2}f'_{\lambda\ell}(\xi)+\xi^{\ell+1}e^{-\xi^2/2}f''_{\lambda\ell}(\xi)$$
$$+\xi^{\ell+3}e^{-\xi^2/2}f_{\lambda\ell}(\xi), \tag{10.136}$$

and substitute the result into Eq. (10.134) arrive at

$$\xi f''_{\lambda\ell}(\xi)+2\left[(\ell+1)-\xi^2\right]f'_{\lambda\ell}(\xi)+[\lambda-3-2\ell]\,\xi f_{\lambda\ell}(\xi)=0. \tag{10.137}$$

In contrast to Eq. (10.94) for the hydrogen atom problem, the quantity ξ^2 appears rather than ξ in the factor multiplying $f'_{\lambda\ell}(\xi)$. With the replacements

$$y=\xi^2, \tag{10.138a}$$
$$\frac{d}{d\xi}=2\xi\frac{d}{dy}=2\sqrt{y}\frac{d}{dy}; \tag{10.138b}$$
$$\frac{d^2}{d\xi^2}=2\frac{d}{dy}+4\xi\sqrt{y}\frac{d^2}{dy^2}=2\frac{d}{dy}+4y\frac{d^2}{dy^2}; \tag{10.138c}$$
$$f_{\lambda\ell}(\xi)\to g_{\lambda\ell}(y), \tag{10.138d}$$

Eq. (10.137) is transformed into

$$yg''_{\lambda\ell}(y)+\left[\left(\ell+\frac{3}{2}\right)-y\right]g'_{\lambda\ell}(y)+\left[\frac{\lambda-3-2\ell}{4}\right]g_{\lambda\ell}(y)=0, \tag{10.139}$$

which is Laguerre's equation. For physically acceptable solutions, it is necessary that

$$\frac{\lambda-3-2\ell}{4}=q \tag{10.140}$$

where q is a positive integer or zero and

$$\alpha=\ell+\frac{3}{2}>-1. \tag{10.141}$$

The condition on α is satisfied automatically, while the condition on λ is

$$\lambda=(4q+2\ell)+3=2n+3, \tag{10.142}$$

or, using Eq. (10.133),

$$E_n=\left(n+\frac{3}{2}\right)\hbar\omega, \tag{10.143}$$

where

$$n = 2q + \ell, \tag{10.144}$$

which implies that $n = \ell, \ell + 2, \ell + 4, \ldots$ Alternatively, for a given $n \geq 0$, $\ell = n, n-2, \ldots$, with the minimum value of ℓ equal to zero if n is even and one if n is odd. Thus

$$\ell = 0, 2, 4, \ldots, n \qquad n \text{ even} \tag{10.145a}$$

$$\ell = 1, 3, 5, \ldots, n \qquad n \text{ odd}. \tag{10.145b}$$

Since there are $(2\ell + 1)$ degenerate substates for each ℓ, you can verify easily that the degeneracy of a state of given n is $(n + 1)(n + 2)/2$, as was found previously using rectangular coordinates. There is an "accidental" degeneracy, as in hydrogen, owing to the fact that the classical orbits are closed ellipses, but, in contrast to hydrogen, all degenerate states have the same parity. This is connected with the fact that the Lenz vector for the Coulomb problem does not commute with the parity operator, but the Lenz "vector" (actually a second rank tensor consisting of five operators) for the harmonic oscillator does commute with the parity operator. The symmetry group for the oscillator is $SU(3)$, the special unitary group in three dimensions.

The physically acceptable solution of Eq. (10.139) is

$$g_{n\ell}(y) = L^{(\ell+\frac{1}{2})}_{(\frac{n-\ell}{2})}(y) \tag{10.146}$$

or

$$f_{n\ell}(\xi) = L^{(\ell+\frac{1}{2})}_{(\frac{n-\ell}{2})}\left(\xi^2\right). \tag{10.147}$$

As a consequence, I can write the normalized (dimensionless) radial wave functions as

$$\tilde{R}_{n\ell}(\xi) = \sqrt{\frac{2}{\xi}}\Lambda^{(\ell+\frac{1}{2})}_{(\frac{n-\ell}{2})}\left(\xi^2\right) \tag{10.148}$$

$$= \sqrt{2}\frac{\left[\left(\frac{n-\ell}{2}\right)!\right]^{1/2}}{\left[\Gamma\left(\frac{n+\ell+3}{2}\right)\right]^{1/2}}\xi^{\ell}e^{-\xi^2/2}L^{(\ell+\frac{1}{2})}_{(\frac{n-\ell}{2})}\left(\xi^2\right), \tag{10.149}$$

where Λ^{α}_{q} is defined by Eq. (10.169) and Γ is the gamma function defined by

$$\Gamma(x) = \int_0^{\infty} t^{x-1}e^{-t}dt, \tag{10.150}$$

such that $\Gamma(n+1) = n!$ for integers $n \geq 0$. The first few dimensionless radial wave functions are

$$\tilde{R}_{00}(\xi) = \frac{2}{\pi^{1/4}} e^{-\xi^2/2}; \tag{10.151a}$$

$$\tilde{R}_{11}(\xi) = \frac{2}{\pi^{1/4}} \sqrt{\frac{2}{3}} \xi e^{-\xi^2/2}; \tag{10.151b}$$

$$\tilde{R}_{20}(\xi) = \frac{2}{\pi^{1/4}} \sqrt{\frac{2}{3}} \left(\frac{3}{2} - \xi^2\right) e^{-\xi^2/2}; \tag{10.151c}$$

$$\tilde{R}_{22}(\xi) = \frac{2}{\pi^{1/4}} \sqrt{\frac{4}{15}} \xi^2 e^{-\xi^2/2}. \tag{10.151d}$$

The radial wave functions in coordinate space are given by

$$R_{n\ell}(r) = \left(\frac{\mu\omega}{\hbar}\right)^{3/4} \tilde{R}_{n\ell}\left(\sqrt{\frac{\mu\omega}{\hbar}} r\right). \tag{10.152}$$

Qualitatively, the results are similar to those for the hydrogen atom, since the orbits are elliptical in both cases; however, the radial coordinate is a minimum on the semi-*minor* axis rather than the semi-major axis of the ellipse, since the center of force is at the origin in the case of the oscillator whereas it is at one of the foci in the Coulomb problem. The (dimensionless) radial probability distribution is

$$\tilde{P}_{n\ell}(\xi) = \xi^2 \tilde{R}^2_{n\ell}(\xi) = \frac{2\xi^{2(\ell+1)} e^{-\xi^2} \left[L^{(\ell+\frac{1}{2})}_{(\frac{n-\ell}{2})}\left(\xi^2\right)\right]^2 \left(\frac{n-\ell}{2}\right)!}{\Gamma\left[\frac{n}{2} + \frac{\ell}{2} + \frac{3}{2}\right]}. \tag{10.153}$$

The maximum of $\tilde{P}_{n,n}(\xi)$ (which corresponds most closely to circular orbits) occurs at $\xi_{\max} = \sqrt{(n+1)}$, the prediction of Eq. (10.128) of the Bohr theory of the oscillator. In contrast to hydrogen, $\xi_{\max}$ grows much more slowly with increasing n (as $\sqrt{n+1}$ rather than as n^2) owing to the fact that the binding force is much stronger for the oscillator than for the electron in hydrogen.

For the oscillator, it follows from Eqs. (10.5) and (10.7) that

$$T_{21} = \frac{T}{4} = \frac{\pi}{2\omega}, \tag{10.154}$$

where T is the period of the classical orbit. As a consequence, the classical radial probability distribution in dimensionless units, obtained from Eqs. (10.6) and (10.7), is

$$\tilde{P}_{n\ell}^{\text{class}}(\xi) = \sqrt{\frac{\hbar}{\mu\omega}} P^{\text{class}}\left(\sqrt{\frac{\hbar}{\mu\omega}}\xi\right)$$
$$= \frac{2}{\pi\sqrt{2n+3-\xi^2-\frac{\ell(\ell+1)}{\xi^2}}}, \tag{10.155}$$

where the argument of the square root is restricted to positive values and I have set $E = \left(n + \frac{3}{2}\right)\hbar\omega$, $L^2 = \hbar^2\ell\,(\ell+1)$. For $\ell = n \gg 1$ (which corresponds most closely to circular orbits), the distribution $\tilde{P}_{n\ell}^{\text{class}}(\xi)$ is confined to a small range about $\xi = \sqrt{n+1}$, as is the quantum probability distribution. For $\ell = 0$, the classical radial probability distribution extends to the center of force and there is a turning point at $\xi = \sqrt{2n+3}$. As in the Coulomb problem, the classical radial probability agrees very well with the quantum distribution, averaged over oscillations, in the classically allowed region. Comparisons are left to the problems.

10.7 Summary

The Schrödinger equation for problems with spherical symmetry can be reduced to a one-dimensional equation for the radial wave function. I have solved the radial equation for a number of problems involving spherically symmetric potentials. It is fortuitous that the solution of the spherical well potential, the Coulomb potential, and the isotropic oscillator potential can be written in terms of known functions. In most cases, it is necessary to solve the radial equation numerically. To help interpret the results, I made comparisons of the quantum probability distributions with the corresponding classical distributions.

10.8 Appendix: Laguerre Polynomials

Laguerre's equation

$$yf''(y) + [\alpha + 1 - y]f'(y) + qf(y) = 0 \tag{10.156}$$

admits polynomial solutions of order q when q is a positive integer or zero and $\alpha > -1$. The solutions of this equation with these restrictions are the generalized Laguerre polynomials

$$f(y) = L_q^{\alpha}(y). \tag{10.157}$$

If these conditions are not met, the solutions of Eq. (10.156) are not convergent in the interval $(0, \infty)$ and do not enter as physically acceptable solutions in the problems I am considering.

Some equations related to Eq. (10.156) and their appropriate solutions are

$$yf''(y) + [y+1]f'(y) + \left(q + \frac{\alpha}{2} + 1 - \frac{\alpha^2}{4y}\right)f(y) = 0; \tag{10.158a}$$

$$f = e^{-y}y^{\alpha/2}L_q^\alpha(y); \tag{10.158b}$$

$$f''(y) + \left(\frac{q + (\alpha+1)/2}{y} + \frac{1-\alpha^2}{4y^2} - \frac{1}{4}\right)f(y) = 0; \tag{10.159a}$$

$$f = e^{-y/2}y^{(\alpha+1)/2}L_q^\alpha(y); \tag{10.159b}$$

$$f''(y) + \left(4q + 2\alpha + 2 - y^2 + \frac{\frac{1}{4} - \alpha^2}{y^2}\right)f(y) = 0; \tag{10.160a}$$

$$f = e^{-y^2/2}y^{\alpha+1/2}L_q^\alpha(y^2). \tag{10.160b}$$

Some properties of the generalized Laguerre polynomials are listed below:
The orthogonality of the generalized Laguerre polynomials is expressed as

$$\int_0^\infty dy L_q^\alpha(y)L_{q'}^\alpha(y)e^{-y}y^\alpha = \frac{\Gamma(q+\alpha+1)}{q!}\delta_{q,q'}, \tag{10.161}$$

where

$$\Gamma(x) = \int_0^\infty t^{x-1}e^{-t}dt \tag{10.162}$$

is the gamma function; a series expansion is

$$L_q^\alpha(y) = \sum_{m=0}^{q}\binom{q+\alpha}{q-m}\frac{(-y)^m}{m!}, \tag{10.163}$$

where the binomial coefficient is defined as

$$\binom{a}{b} = \frac{\Gamma(a+1)}{\Gamma(b+1)\Gamma(a-b+1)}; \tag{10.164}$$

the generating function is

$$F(y,h) = \frac{1}{(1-h)^{\alpha+1}}e^{-\frac{hy}{1-h}} = \sum_{q=0}^{\infty}L_q^\alpha(y)h^q; \tag{10.165}$$

the identity

$$\frac{d}{dy}L_{q+1}^{\alpha}(y) = -L_q^{\alpha+1}(y) = \frac{1}{y}\left[(q+1)\,L_{q+1}^{\alpha}(y) - (q+1+\alpha)\,L_q^{\alpha}(y)\right] \tag{10.166}$$

and the fact that $L_0^{\alpha}(y) = 1$ can be used to generate all the generalized Laguerre polynomials; the first few generalized Laguerre polynomials are

$$L_0^{\alpha}(y) = 1; \tag{10.167a}$$

$$L_1^{\alpha}(y) = -y + \alpha + 1; \tag{10.167b}$$

$$L_2^{\alpha}(y) = \frac{1}{2}\left[y^2 - 2\,(\alpha+2)\,y + (\alpha+1)\,(\alpha+2)\right]; \tag{10.167c}$$

a useful recursion relation is

$$(q+1)\,L_{q+1}^{\alpha}(y) - (2q+\alpha+1-y)\,L_q^{\alpha}(y) + (q+\alpha)\,L_{q-1}^{\alpha}(y) = 0. \tag{10.168}$$

The associated Laguerre functions defined by

$$\Lambda_q^{\alpha}(y) = \sqrt{\frac{q!}{\Gamma\,(q+\alpha+1)}}e^{-y/2}y^{\alpha/2}L_q^{\alpha}(y) \tag{10.169}$$

satisfy the orthogonality relations

$$\int_0^{\infty} dy\Lambda_q^{\alpha}(y)\Lambda_{q'}^{\alpha}(y) = \delta_{q,q'}; \tag{10.170}$$

$$2\left(\frac{1}{n^3n'^3}\right)^{1/2}\int_0^{\infty} d\rho\,\rho\Lambda_{n-\ell-1}^{2\ell+1}\left(\frac{2\rho}{n}\right)\Lambda_{n'-\ell-1}^{2\ell+1}\left(\frac{2\rho}{n'}\right) = \delta_{n,n'}, \tag{10.171}$$

and the recursion relation

$$\begin{aligned}\sqrt{(q+1)\,(q+\alpha+1)}\Lambda_{q+1}^{\alpha}(y) - (2q+\alpha+1-y)\,\Lambda_q^{\alpha}(y)\\ +\sqrt{q\,(q+\alpha)}\Lambda_{q-1}^{\alpha}(y) = 0.\end{aligned} \tag{10.172}$$

10.9 Problems

1. Find the three lowest energy states in electron volts for the $\ell = 0$ and $\ell = 1$ states of a particle having mass $\mu = 10^{-30}$ kg moving in an *infinite*, spherical potential well having radius $a = 10^{-9}$ m.

2. A particle having mass μ moves in a spherical well potential

$$V(r) = \begin{cases} -V_0 < 0 & r < a \\ 0 & r > a \end{cases}.$$

The lowest energy state has $\ell = 0$. Find the value of V_0 needed to guarantee a bound state. How does this problem differ from a three-dimensional square well potential, for which a bound state always exists?

3. Draw the effective potential for the potential of Problem 10.2. For a given energy, find values of the angular momentum for which bound states can exist classically. Classically, can bound states exist for $E > 0$? Explain. In the quantum problem, can bound states exist for $E > 0$? Explain. Find a condition on ℓ in the quantum problem that will guarantee that a bound state cannot exist.

4–5. For the potential of Problem 10.2, calculate the eigenenergies for $\ell = 1$ and $\beta = 2, 4, 6$, where $\beta = \sqrt{2\mu V_0 a^2/\hbar^2}$. In each case express the eigenenergies in terms of the dimensionless quantity $x = \kappa a = \sqrt{-2\mu E a^2/\hbar^2}$. You will have to solve Eq. (10.79) graphically to obtain the solutions. Classically, what is the minimum value of β needed to have a bound state with $E < 0$ for an angular momentum $L = \hbar\sqrt{\ell(\ell+1)}$ and $\ell = 1$? How does this compare with the minimum value of β needed to support a bound state in the quantum problem?

6. Give a very rough uncertainty principle argument to estimate the ground state energy of hydrogen. To do this replace $\langle 1/r \rangle$ by $1/\langle r \rangle$ and set $\langle p_r^2 \rangle = \hbar^2/\left(4\langle r \rangle^2\right)$ in $\left\langle \hat{H} \right\rangle$.

7. Using the effective potential for hydrogen,

$$V_{\text{eff}} = -\frac{K_e}{r} + \frac{\hbar^2 \ell(\ell+1)}{2\mu r^2},$$

where $K_e = e^2/4\pi\epsilon_0$, show that, for fixed

$$E = -\frac{1}{2}\mu c^2 \left(\frac{K_e^2}{\hbar^2 c^2}\right)\frac{1}{n^2} < 0,$$

there is a maximum value of ℓ allowed and that it corresponds *roughly* to what is found in the quantum theory, that is to $\ell_{\max} = n - 1$.

8. Plot the dimensionless radial probability distribution, $\rho^2 \left|\tilde{R}_{n\ell}(\rho)\right|^2$, for the $n = 2, \ell = 1$; $n = 2, \ell = 0$; $n = 10, \ell = 9$; $n = 10, \ell = 5$; and $n = 10, \ell = 0$ states of the hydrogen atom. Interpret your results.

9. Use the recursion relation

$$\rho\Lambda_{n-\ell-1}^{2\ell+1}(\rho) = 2n\Lambda_{n-\ell-1}^{2\ell+1}(\rho) - \sqrt{(n+\ell+1)(n-\ell)}\Lambda_{n-\ell}^{2\ell+1}(\rho) - \sqrt{(n-\ell-1)(n+\ell)}\Lambda_{n-\ell-2}^{2\ell+1}(\rho)$$

to derive

$$\langle\rho\rangle = \int_0^\infty \rho\tilde{P}_{n\ell}(\rho) = \frac{3n^2 - \ell(\ell+1)}{2},$$

where $\tilde{P}_{n\ell}(\rho)$ is the dimensionless radial probability distribution for the electron in hydrogen.

10. Construct a "Bohr theory" for the 3-D isotropic harmonic oscillator and show that the maximum of the quantum radial probability distribution for the oscillator agrees with your theory for states having $n = \ell$.

11. Plot the dimensionless radial probability distribution $\tilde{P}_{n\ell}(\xi)$ for the $n = 60$, $\ell = 60, 30, 0$ states of the 3-D isotropic harmonic oscillator given in Eq. (10.153), along with the classical distribution given by Eq. (10.155). Interpret your results.

12. Prove that the wave function for the 3-D isotropic harmonic oscillator is periodic and that $\langle\mathbf{r}\rangle$ obeys the classical equation of motion for the oscillator. Does the *radial* motion oscillate at frequency ω? Explain.

13–14. Consider the $n = 2$ state of the 3-D isotropic oscillator. Write the dimensionless wave functions in both rectangular and spherical coordinates. Write each of the rectangular wave functions in terms of the eigenfunctions in spherical coordinates.

15–16. In cylindrical coordinates (ρ, ϕ), the Hamiltonian for a particle having mass μ moving in a potential $V(\rho)$ is

$$\begin{aligned}\hat{H} &= -\frac{\hbar^2}{2\mu}\nabla^2 + V(\rho) \\ &= -\frac{\hbar^2}{2\mu}\left(\frac{1}{\rho}\frac{\partial}{\partial\rho}\rho\frac{\partial}{\partial\rho} + \frac{1}{\rho^2}\frac{\partial^2}{\partial\phi^2}\right) + V(\rho).\end{aligned}$$

The angular momentum operator is $\hat{L}_z = \frac{\hbar}{i}\frac{\partial}{\partial\phi}$, so the Hamiltonian can be written as

$$\begin{aligned}\hat{H} &= -\frac{\hbar^2}{2\mu}\left(\frac{1}{\rho}\frac{\partial}{\partial\rho}\rho\frac{\partial}{\partial\rho} - \frac{\hat{L}_z^2}{\hbar^2\rho^2}\right) + V(\rho) \\ &= -\frac{\hbar^2}{2\mu}\left(\frac{1}{\rho}\frac{\partial}{\partial\rho}\rho\frac{\partial}{\partial\rho}\right) + \frac{\hat{L}_z^2}{2\mu\rho^2} + V(\rho).\end{aligned}$$

On the other hand, the classical Hamiltonian is

$$H_{\text{class}} = \frac{p_\rho^2}{2\mu} + \frac{L_z^2}{2\mu\rho^2} + V(\rho) = \frac{p_\rho^2}{2\mu} + V_{\text{eff}},$$

where $p_\rho = \mathbf{p} \cdot \mathbf{u}_\rho$. This would suggest that

$$\hat{p}_\rho^2 = -\hbar^2 \left(\frac{1}{\rho} \frac{\partial}{\partial \rho} \rho \frac{\partial}{\partial \rho} \right)$$

and

$$V_{\text{eff}} = \frac{\hat{L}_z^2}{2\mu\rho^2} + V(\rho),$$

but this is **not** the case. To prove this show that $\hat{p}_\rho$ defined as

$$\begin{aligned} \hat{p}_\rho &= \frac{1}{2} \left(\hat{\mathbf{p}} \cdot \mathbf{u}_\rho + \mathbf{u}_\rho \cdot \hat{\mathbf{p}} \right) \\ &= \frac{\hbar}{2i} \left(\boldsymbol{\nabla} \cdot \mathbf{u}_\rho + \mathbf{u}_\rho \cdot \boldsymbol{\nabla} \right) \end{aligned}$$

is equal to

$$\hat{p}_\rho = \frac{\hbar}{i} \left(\frac{\partial}{\partial \rho} + \frac{1}{2\rho} \right)$$

and that

$$\hat{p}_\rho^2 = -\hbar^2 \left(\frac{1}{\rho} \frac{\partial}{\partial \rho} \rho \frac{\partial}{\partial \rho} \right) + \frac{\hbar^2}{4\rho^2}.$$

As a consequence show that, in the quantum problem,

$$V_{\text{eff}} = \frac{\hat{L}_z^2}{2\mu\rho^2} - \frac{\hbar^2}{8\mu\rho^2} + V(\rho).$$

In other words, there is an attractive "barrier" in the 2-D problem, even for eigenfunctions corresponding to $\left\langle \hat{L}_z^2 \right\rangle = 0$. This is the reason why there is always a bound state for a "circular" potential well in two dimensions.

17. The Hamiltonian for the previous problem is

$$\hat{H} = -\frac{\hbar^2}{2\mu} \left(\frac{1}{\rho} \frac{\partial}{\partial \rho} \rho \frac{\partial}{\partial \rho} + \frac{1}{\rho^2} \frac{\partial^2}{\partial \phi^2} \right) + V(\rho).$$

Assume a solution for the eigenfunctions of the form

$$\psi_{Em}(\boldsymbol{\rho}) = u_{Em}(\rho)e^{im\phi}/\sqrt{\rho},$$

where m is an integer, and show that the radial equation for $u_{Em}(\rho)$ is

$$u''_{Em}(\rho) + \left[\frac{2\mu}{\hbar^2}\left[E - V(\rho)\right] + \frac{1-4m^2}{4\rho^2}\right]u_{Em}(\rho) = 0.$$

For the potential $V(\rho) = \mu\rho^2\omega^2/2$ (isotropic two-dimensional harmonic oscillator), introduce dimensionless variables

$$\xi = \sqrt{\frac{\mu\omega}{\hbar}}\rho; \quad \lambda = 2E/\hbar\omega,$$

and show that the dimensionless radial function $\tilde{u}_{\lambda m}(\xi)$ obeys the differential equation

$$\tilde{u}''_{\lambda m}(\xi) + \left(\lambda + \frac{\left(1-4m^2\right)}{4\xi^2} - \xi^2\right)\tilde{u}_{\lambda m}(\xi) = 0.$$

Compare this with Eq. (10.160) to show that the eigenenergies are

$$E_n = (n+1)\hbar\omega; \quad n = 0, 1, 2, \ldots.$$

and that the dimensionless radial eigenfunctions are

$$\tilde{R}_{nm}(\xi) = \sqrt{2\frac{\left(\frac{n-|m|}{2}\right)!}{\left(\frac{n+|m|}{2}\right)!}}\xi^{|m|}e^{-\xi^2/2}L^{|m|}_{\frac{n-|m|}{2}}(\xi^2),$$

where m varies from $-n$ to n in integer steps of 2.

18–19. The classical Hamiltonian for a particle having mass μ and charge q moving in a constant magnetic field $\mathbf{B}$ is given by

$$H = \frac{(\mathbf{p} - q\mathbf{A})^2}{2\mu}$$

where

$$\mathbf{A} = -\mathbf{r} \times \mathbf{B}/2$$

is the vector potential. Prove that $\mathbf{B} = \nabla \times \mathbf{A}$ and show that the Hamiltonian can be written as

$$H = \frac{p^2}{2\mu} - \frac{q\mathbf{L}\cdot\mathbf{B}}{2\mu} + \frac{A^2}{2\mu},$$

where $\mathbf{L} = \mathbf{r} \times \mathbf{p}$ and $\mathbf{p}$ is the canonical momentum, related to the velocity by

$$\mathbf{p} = \mu\dot{\mathbf{r}} + q\mathbf{A}.$$

If the initial velocity is perpendicular to $\mathbf{B}$, prove that the motion is in a plane perpendicular to $\mathbf{B}$.

Now assume that the magnetic field is along the z-direction, $\mathbf{B} = B\mathbf{u}_z$ and consider the motion to be confined in the xy plane. Use cylindrical coordinates (ρ, ϕ). At $t = 0$, take

$$\boldsymbol{\rho}(0) = \boldsymbol{\rho}_0 = x_0\mathbf{u}_x + y_0\mathbf{u}_y;$$
$$\mathbf{v}(0) = \mathbf{v}_0 = v_{x0}\mathbf{u}_x + v_{y0}\mathbf{u}_y.$$

Use the Lorentz force equation to find $\mathbf{v}(t)$ and integrate the result to obtain $\boldsymbol{\rho}(t)$. Prove that the orbit of the particle is a circle of radius $R = v_0/\omega_c$ centered at

$$x_c = x_0 + v_{y0}/\omega_c;$$
$$y_c = y_0 - v_{x0}/\omega_c,$$

where

$$\omega_c = \frac{qB}{\mu}$$

is the *cyclotron frequency*. Prove the following relationships:

$$H = \frac{1}{2}\mu v(t)^2 = \text{constant} = \frac{1}{2}\mu v_0^2;$$
$$L_z = \text{constant} = |\boldsymbol{\rho}_0 \times \mathbf{p}_0| = \mu\left(x_0 v_{0y} - y_0 v_{0x}\right) + \omega_c\rho_0^2/2$$
$$= \omega_c\rho_c^2/2;$$
$$H = \frac{1}{2}\mu\dot{\rho}\,(t)^2 + V_{\text{eff}}(\rho),$$

where

$$\boldsymbol{\rho}(t) = x(t)\mathbf{u}_x + y(t)\mathbf{u}_y = \rho(t)\mathbf{u}_\rho;$$
$$\rho_c^2 = x_c^2 + y_c^2;$$

$$\mathbf{v}(t) = \dot{\boldsymbol{\rho}}(t) = v_x(t)\mathbf{u}_x + v_y(t)\mathbf{u}_y = \dot{\rho}\,(t)\,\mathbf{u}_\rho + \rho(t)\dot{\phi}(t)\mathbf{u}_\phi;$$

$$V_{\text{eff}}(\rho) = \frac{L_z^2}{2\mu\rho^2} - \frac{qL_zB}{2\mu} + \frac{q^2B^2}{8\mu}\rho^2.$$

Note that the distance from the origin to the center of the orbit scales as $\sqrt{L_z}$.

20–21. Now consider the corresponding quantum problem with the magnetic field in the z-direction, for which

$$\hat{H} = \frac{\left(\hat{\mathbf{p}} - q\hat{\mathbf{A}}\right)^2}{2\mu}$$

$$= \frac{\hat{p}^2}{2\mu} + \frac{q^2B^2}{8\mu}\rho^2 - \frac{q\hat{L}_zB}{2\mu}$$

(the fact that $\hat{p}_j$ commutes with $\hat{A}_j$ is needed to arrive at this result). Show that the Hamiltonian is the same as that for an isotropic two-dimensional harmonic oscillator having frequency

$$\omega = \frac{\omega_c}{2} = \frac{qB}{2\mu},$$

except that there is an *additional term*,

$$-\frac{q\hbar mB}{2\mu} = -m\hbar\omega,$$

in the radial equation. As a consequence of this term, show that the equation for the radial function u_{Em} of problem 10.17 acquires an additional term, $2mu_{Em}$, and then use the results of of problem 10.17 to show that the energy levels are given by

$$E_n = \left(n + \frac{1}{2}\right)\hbar\omega_c,$$

where n is an integer ≥ 0 and m is an integer that ranges from $-n$ to infinity. Thus, there is an *infinite* degeneracy for each n, a result that can be traced to the translational symmetry of the problem. Use the effective potential to show why this degeneracy is possible for this problem, but not for the isotropic two-dimensional oscillator. The equally spaced n levels for this potential are referred to as *Landau levels* (after Lev Landau). Obtain the radial eigenfunctions and plot the dimensionless radial probability distribution for $n = 10$ and $m = 100, 400$ on the same graph. Check to see if changing the value of m results in a translation of the probability distribution and if the radial position of the center of the distribution scales approximately as $\sqrt{m}$, as predicted from classical considerations.